Link Adaptation Techniques
for
Cellular Fixed Broadband Wireless Access Systems

By

Ehab Armanious

A thesis submitted to
The Faculty of Graduate Studies and Research
in partial fulfillment of the requirements
for the degree of
Master's of Applied Science (Electrical Engineering)

Ottawa-Carleton Institute for Electrical and Computer Engineering
Department of Systems and Computer Engineering
Carleton University
Ottawa, Canada
January 2003

The undersigned herby recommended to the Faculty of Graduate Studies and Research acceptance of the thesis

Link Adaptation Techniques
for
Cellular Fixed Broadband Wireless Access Systems

Submitted by Ehab Armanious

in partial fulfillment of the requirements

for the degree of

Master's of Applied Science (Electrical Engineering)

Thesis Supervisor

Professor Halim Yanikomeroglu

Thesis Co-Supervisor

Professor David Falconer

Chair, Department of Systems and Computer Engineering

Carleton University
2003

Abstract

Adaptive modulation, error control coding and power control are well-known techniques that have been applied to mobile wireless communication systems. These techniques, when designed to track the channel variations, yield a higher network throughput. In this research, we investigate the throughput returns due to the employments of various combinations of adaptive modulation, adaptive coding, and adaptive power control in a broadband fixed wireless access cellular system. We take into account the effects of shadowing, Multipath fading, and multiple access interference. The system considered is Multipoint Multichannel Distribution System (MMDS) with carrier frequency 2.5 GHz. We found that among all the possible combinations, the combination of adaptive modulation and adaptive coding (without power control) is the most efficient type since combining adaptive power control with the first two techniques adds a relatively small improvement in the throughput.

Acknowledgement

I wish to express my sincere gratitude to my supervisor, Professor Halim Yanikomeroglu, and my co-supervisor, Professor David Falconer, for their guidance and patience over the course of my thesis research. The suggested approaches provided by Professor Ian Marsland to solve some of the problems that were encountered in the simulation are greatly appreciated.

Many thanks are also due to Dr. Gamantyo Hendrantoro of Jurusan Teknik Elektro, Institut Teknologi Sepuluh Nopember, Surabaya, Indonesia for providing constructive feedback on several issues. I am grateful for the technical support provided by Mr. Narendra Mehta. I wish to thank my fellow graduate students and the staff of the Department of Systems and Computer Engineering for their continuous help and support.

I am thankful to Dr. Sirikiat Lek Ariyavisitakul of Radia Communications, Norcross, GA, USA, for providing several performance curves, which accelerated my research and helped me focus on the analysis and development of my thesis.

I am also grateful to The Canadian Institute for Telecommunication Research (CITR) for funding this research.

Table of Content

List of Figures

List of Tables

List of Acronyms

AWGN: Additive White Gaussian Noise.

BS: Base Station.

CPE: Customer Premises Equipment.

UL: Uplink direction (CPE to BS).

DL: Downlink direction (BS to CPE).

BER: Bit Error Rate.

FER: Frame Error Rate.

SINR: Signal to Interference plus Noise Ratio.

CDMA: Code-Division Multiple Access.

TDMA: Time-Division Multiple Access.

TDM: Time Division Multiplexing.

QoS: Quality of Service.

FDD: Frequency Division Duplex.

MMDS: Multipoint Multichannel Distribution System.

NLOS: Non Line of Sight.

AM: Adaptive Modulation.

AC: Adaptive Coding.

PC: Power Control.

List of Symbols

f_c: The carrier frequency.

$T_x BW$: The transmission bandwidth.

k: The Rician Parameter.

2β : The antenna beamwidth.

G_s: The side lobe gain of the antenna.

G_m: The main lobe gain of the antenna.

G_t: The transmitting antenna gain ratio.

Gr: The receiving antenna gain ratio.

α : The angle of arrival from the BS to the CPE.

θ : The angle between the serving BS and the vertical axis (see section 3.3)

ϕ : The angle between the interfering BS and the vertical axis (see section 3.3)

I: The received Interference.

S: The received signal of interest.

d_o: The reference distance from the BS.

d: The user's distance from the BS.

c: The speed of light.

n: the propagation exponent.

K; Boltzman's constant

T^o: Ambient temperature.

W: The transmission bandwidth.

N: the thermal noise.

Chapter 1: Introduction

1.1 Thesis Objectives

Wireless communications have experienced significant advances in recent years. Several techniques have been tried in order to improve the performance. Fixed cellular communication is a segment of the wireless communication technology where subscribers are located at fixed positions with respect to the base station. The increased demand to provide communication services to fixed users in an efficient and cost effective manner compared with wireline-based communication systems has triggered myriad research activities for fixed wireless communication systems.

Wireless communication systems suffer from several shortcomings introduced by the environment such as shadowing and fading. In order to provide reliable services with the required data rates, several techniques will be examined in this thesis.

Reliability and high throughput are considered two important factors for a successful deployment of any fixed wireless communication system since these factors are already available for wireline communication systems. In order to achieve these goals in a wireless communication system, where time varying channels are always present, some techniques will be tried in order to track the channel as close as possible.

The main objective of this thesis is to investigate the advantage of using different combinations of adaptive modulation, adaptive coding and power control in order to increase the throughput of the system. Fixed wireless communication systems are expected to provide services such as broadband Internet and digital TV. These services

require data rates that are higher in the downlink (the base station to the subscriber equipment) than those in the uplink (the subscriber equipment to the base station). Therefore, this thesis will focus on improving the throughput of the downlink direction.

Since line of sight is not always available for wireless communications systems due to foliage, buildings, and obstructing objects, a non-line of sight system is considered in the research. The non-line of sight system is represented by a propagation exponent of 4.

1.2 Thesis Organization

This thesis is organized as follows: Chapter 2 reviews the state of the art in the area of fixed wireless communication systems. The coding scheme used in the thesis is Bit-Interleaved Coded Modulation (BICM). An overview of BICM is provided in chapter 2. An overview of power control and adaptive modulation is also presented in chapter 2. We also examine how the previous research activities used modulation, coding and power coding techniques.

Chapter 3 presents the research problem under analysis in this thesis. We begin with the statement of the thesis question. Then we justify why this question is significant to address. Direct reference is made to the previous chapter to illustrate that this problem was not handled before in the literature in the manner of this research. The system model is also presented in this chapter.

Due to the significant amount of results available for analysis, we present the results in two chapters. The first part is shown in Chapter 4, where we offer the first part of our thesis results and we argue that adaptive modulation improves the performance and thus is worthwhile for use in fixed wireless communication systems. The second part of the results is provided in Chapter 5; where several combinations of adaptive modulation,

adaptive coding and power control are examined in order to ascertain the most viable performance.

The conclusions, recommendations, and suggestions for future research are given in Chapter 6, where we summarize our findings and state various problems that emerged during the course of our research, which can be used as an impetus for future research.

1.3 Thesis Contributions

This thesis examines the advantage of using adaptive modulation, adaptive coding and power control for fixed cellular wireless access. Several parameters are established to evaluate the advantages of these techniques. The results are summarized as follows:

1. Adaptive modulation alone: It is found that, with any parameter, a fixed wireless access system using adaptive modulation yields throughput higher than any similar system that uses fixed modulation.

2. When power control is combined with adaptive modulation, an incremental improvement is noticed, in addition to the improvement that is provided by using adaptive modulation alone. In addition to the small improvement in the throughput, an appreciable reduction in the average transmitted power is also achieved by controlling the transmitted power.

3. Combining adaptive coding with adaptive modulation provides incremental improvement in the throughput on top of the improvement that is provided by adaptive modulation alone. The incremental improvement is slightly better than the improvement that is achieved by combining power control with adaptive modulation.

4. When adaptive modulation is combined with adaptive coding and power control, the system throughput has shown some further improvement compared to cases 2 and 3.

Chapter 2: Review of Adaptive Techniques and Power Control in Cellular Wireless Communication Systems

2.1 Introduction

In this chapter we present three techniques that have shown increased interest in cellular wireless communication systems namely: adaptive modulation, error control coding and power control. For each technique, we start by presenting the theoretical background for it and then we review the relevant literature.

The wireless channel is characterized by large statistical variations, which results in wide variations in its response. These variations are due to fading and shadowing. If the system is designed to meet the worst-case scenario of the channel, the throughput will be very small and the performance will degrade. On the other hand, if the system is designed to track the channel variations; the throughput will increase and an optimum or near-optimum performance will be obtained. Nanda, Balachandran, and Kumar [1] surveyed several adaptation techniques that are used in various mobile cellular wireless communication systems. These techniques increase the capacity, data rates, and support broader range of services. Babich [2] compares the performance of different adaptive techniques; such as modulation, power, and bit rate; for mobile wireless communication systems that utilizes time-division multiplexing (TDM) scheme in a single-cell and cellular setting. They developed a closed form expression for optimum power and modulation adaptation scheme. The author shows that, in the proposed cellular system, adaptive modulation provides a somewhat better performance compared with power control.

The advantages of applying the above-mentioned techniques in the area of fixed cellular wireless communication systems will be investigated in later chapters.

2.2 Adaptive modulation

Adaptive modulation means changing the constellation size adaptively, according to a specific condition. For wireless communication systems, the component that is varying is the wireless channel. Therefore, the system will select a constellation size that will closely track the channel condition. The channel condition is monitored by the received signal to interference plus noise ratio, SINR, which is defined as follows:

SINR = the received signal power for the user of interest/ (the total received interference power + the received thermal noise power within the operating frequency band).

Figure 1 [40] shows an example for implementing adaptive modulation. The targeted BER is 10^{-5}. The system will choose one of three modulation schemes: 64-QAM, 16-QAM, or QPSK according to the following rule. If the received SINR is larger than or equal to the threshold for 64-QAM, the system will select 64-QAM for modulation. If the received SINR falls in the region between the thresholds of 16-QAM and 64-QAM, the system will select 16-QAM for modulation. Similarly, if the received SINR falls in the region between QPSK and 16-QAM thresholds, the system will select QPSK for modulation. If the received SINR falls anywhere in the region below the threshold for QPSK, the system will not transmit any data until the next measured SINR becomes at least larger than the threshold for QPSK (the smallest threshold).

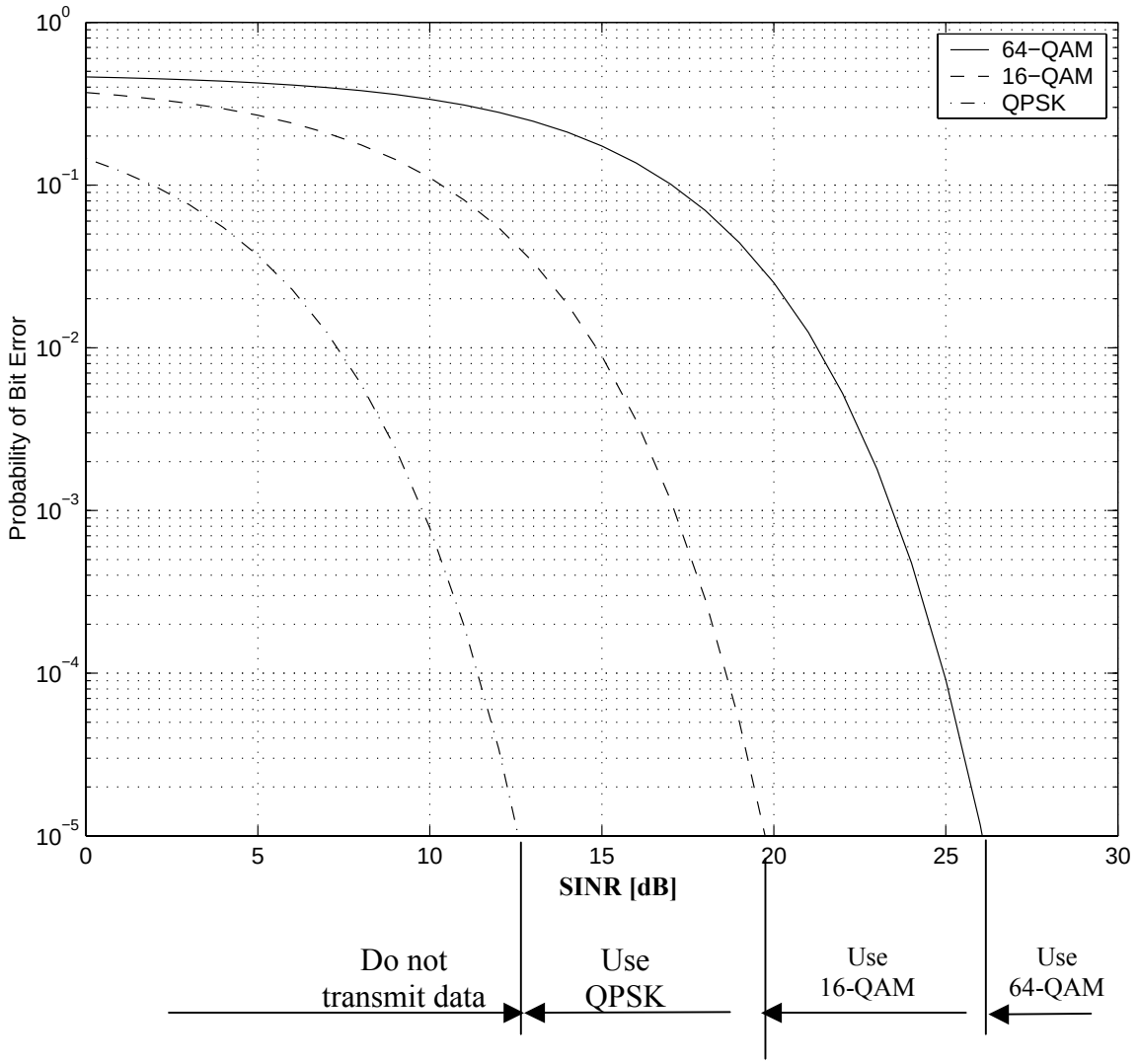

Figure 1: An illustration of the implementation of adaptive modulation (assuming the noise plus the interference have Gaussian distribution)

Implementing adaptive modulation in one side requires feedback information from the other side. For example, if adaptive modulation were to be implemented in the downlink direction, some information has to be sent back in the uplink direction. Figure 2 details a possible approach for implementing adaptive modulation in the downlink direction. This approach can be summarized as follows:

1. The BS sends a training sequence in the down link direction.

2. The CPE evaluates the received SINR from the DL training sequence and sends feedback information to the BS.

3. The BS will evaluate the feedback information that was sent by the CPE and sends the payload with a modulation scheme that matches the current channel condition. The feedback information is assumed to be received correctly by the BS.

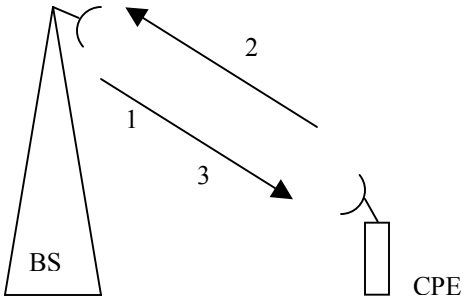

Figure 2: A simplified model for implementing adaptive modulation in the downlink direction

Significant research is conducted to examine the advantage of using adaptive modulation for mobile cellular wireless communication systems. Webb and Steele [3] investigated the advantage of using variable rate QAM for mobile radio channels. They varied the number of modulation levels to track the mobile radio fading channel variations. The fading rate and the block size are considered as parameters. The effect of the co-channel interference on the system performance is also considered. They found that the variable rate system has about 5-dB improvement over a fixed 16-level QAM system for BER's between 10^{-2} and 10^{-5}.

Alouini, Tang, and Goldsmith [4] proposed an adaptive modulation scheme for simultaneous voice and data over fading channels. The scheme dynamically allocates the transmitted power between the in-phase (I) and the quadrature (Q) channels according to

the time-varying nature of the channel. Fixed-rate binary phase shift keying (BPSK) modulation is used on the *Q* channel for voice. Variable-rate M-ary amplitude modulation is used on the *I* channel for data. For favorable channel conditions, most of the power is allocated to high rate data transmission on the *I* channel. The remaining power is used to support the variable-power voice transmission on the *Q* channel. When the channel conditions degrade, the system will allocate sufficient power to *Q* channel, the voice channel; and will allocate the remaining power to channel *I*, the data channel. The authors presented closed-form expressions as well as numerical and simulation results for the outage probability, average allocated power, achievable spectral efficiency, and average bit-error-rate for both voice and data transmission over Nakagami-*m* fading channels.

Hamaguchi, Kamio, and Moriyama [5] presented a system that utilizes adaptive modulation with noticeable characteristics: When the channel conditions degrade to a certain limit, the transmission will stop until the channel improves again. A buffer memory is used to maintain the data transmission rate. They found that the adaptive modulation system provides a noticeable improvement in spectral efficiency and transmission quality.

Kamio, Sampei, Sasaoka, and Norinaga [6] studied the performance of adaptive modulation under limited time delay for land mobile communication systems that operate in Time Division Duplex (TDD) mode. The system selects from a set of four options according to the received SINR. The reciprocity of the propagation path characteristics in the TDD systems is utilized as feedback information about the channel conditions. They show that the proposed method improves the BER performance of a system transmission

data at a constant rate under multi-path fading conditions and the performance is better than that of TCM-32QAM in Rayleigh fading conditions with small Doppler frequency.

Tang, Alouini, and Goldsmith [7] examined the effect of imperfect channel estimates on the BER of multi-level quadrature amplitude modulation (M-QAM). They used pilot symbol assisted modulation (PSAM) to estimate channel fading. Since the decision regions of the demodulator depend on the channel fading, estimation error of the channel variation can severely degrade the demodulator performance. They show that, for 16-QAM and 64-QAM, amplitude estimation error leads to a 1-dB degradation in E_b/N_o and combined amplitude-phase estimation error leads 2.5-dB degradation.

Goldsmith and Chua [8] applied coset codes to adaptive modulation in fading channels. Trellis and lattice codes, which are designed for additive white Gaussian noise (AWGN) channels, are superimposed on adaptive modulation for fading channels, with the same approximate coding gain. By combining coset codes with adaptive modulation techniques, they obtained a coding gain of 3-dB relative to un-coded adaptive MQAM for a simple four-state trellis code, and an effective 3.6-dB coding gain for an eight-state trellis code. They also compared the performance of trellis-coded adaptive MQAM to that of coded modulation with built-in time diversity and fixed-rate modulation. The adaptive method exhibits a power savings of up to 20-dB.

Kim and Lindsey [9] examined the potential improvement in spectral efficiency for slowly fading channels. They used adaptive coded modulation to track the varying channel conditions. They showed that the adaptive coded modulation could provide several folds of increase in spectral efficiency compared to a fixed modulation system employing QPSK when the channel varies slowly.

Ikeda, Sampei, and Norinaga [10] proposed a time-division multiple-access (TDMA)-based adaptive modulation scheme with dynamic channel assignment. The proposed system tries to achieve high-capacity communication system in a dynamically changing path and traffic conditions. The proposed method measures the received carrier-to-noise plus interference power ratio *(C / (N + I))* of each TDMA slot to search available slots as well as to discover the optimum modulation parameters for each terminal. This approach will combine the effect of mitigating both spatially distributed electric field strength variation by the slow adaptive modulation and spatially and temporally distributed traffic variation by the dynamic channel assignment. They argued that the proposed TDMA-based adaptive modulation scheme with dynamic channel assignment system could achieve approximately three times higher system capacity than the conventional fixed channel assignment using QPSK.

2.3 Error Control Coding

The use of error control coding, or channel coding, in broadband fixed cellular wireless systems is investigated in this section. Channel coding represents some techniques of inserting structured redundancy into the source data [12]. This redundancy will be used to reduce the SINR that is required to achieve the same BER, which is essential for an un-coded system. The cost for this improvement is an increase in the required transmission bandwidth for the same data rate or a decrease in the data rate for the same transmission bandwidth. Channel coding can be further divided into block coding and convolutional coding.

Bit-Interleaved Coded Modulation (BICM) was introduced by Zehavi [13] and presented in details in [14]. BICM is a concatenation of convolutional encoder and a modulator. Figure 3 shows a block diagram for implementing BICM. The idea of BICM is to make the Hamming distance, or the code diversity, equal to the smallest number of distinct bits. Reducing the Hamming distance is achieved by performing a bit-wise interleaving process at the output of the convolutional encoder, which will be followed by the modulator. At the receiving end, a soft-decision metric, after the demodulator, is used as an input to a Viterbi decoder.

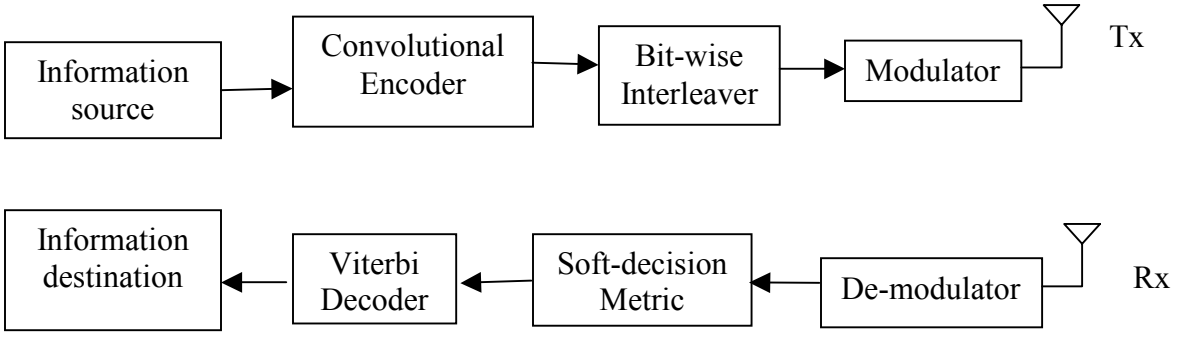

Figure 3: Block Diagram for Bit-Interleaved Coded Modulation (BICM)

The bit-wise Interleaver block, assumed to have an infinite depth, interleaves the

output of the convolutional encoder, i.e. the code sequence. The output of the Interleaver is broken into sequences of bits, which are mapped into signals by the modulator. Ideal bit interleaving is assumed. The authors demonstrated that by separating the modulation/encoding and the demodulation/decoding by bit-wise interleaving, BICM performs very well, especially for high data rates, over fading channels. They also illustrate that Gray coding plays a central role on the performance of BICM.

Using combinations of adaptive modulation and adaptive coding is quite similar to using adaptive modulation alone. Figure 4 illustrates a variety of the possible combinations of adaptive modulation (QPSK, 16-QAM, and 64-QAM) and adaptive BICM (with code rates 1/2, 2/3, 3/4, and 7/8). When adaptive modulation is combined with adaptive coding, the network will have more options to choose from than in the case of using adaptive modulation alone. An expected improvement in the performance will result from these combinations. These curves were obtained from simulations assuming that combinations of adaptive modulation (QPSK, 16-QAM, and 64-QAM) and adaptive BICM (code rates 1/2, 2/3, 3/4, 7/8, and 1) were used.

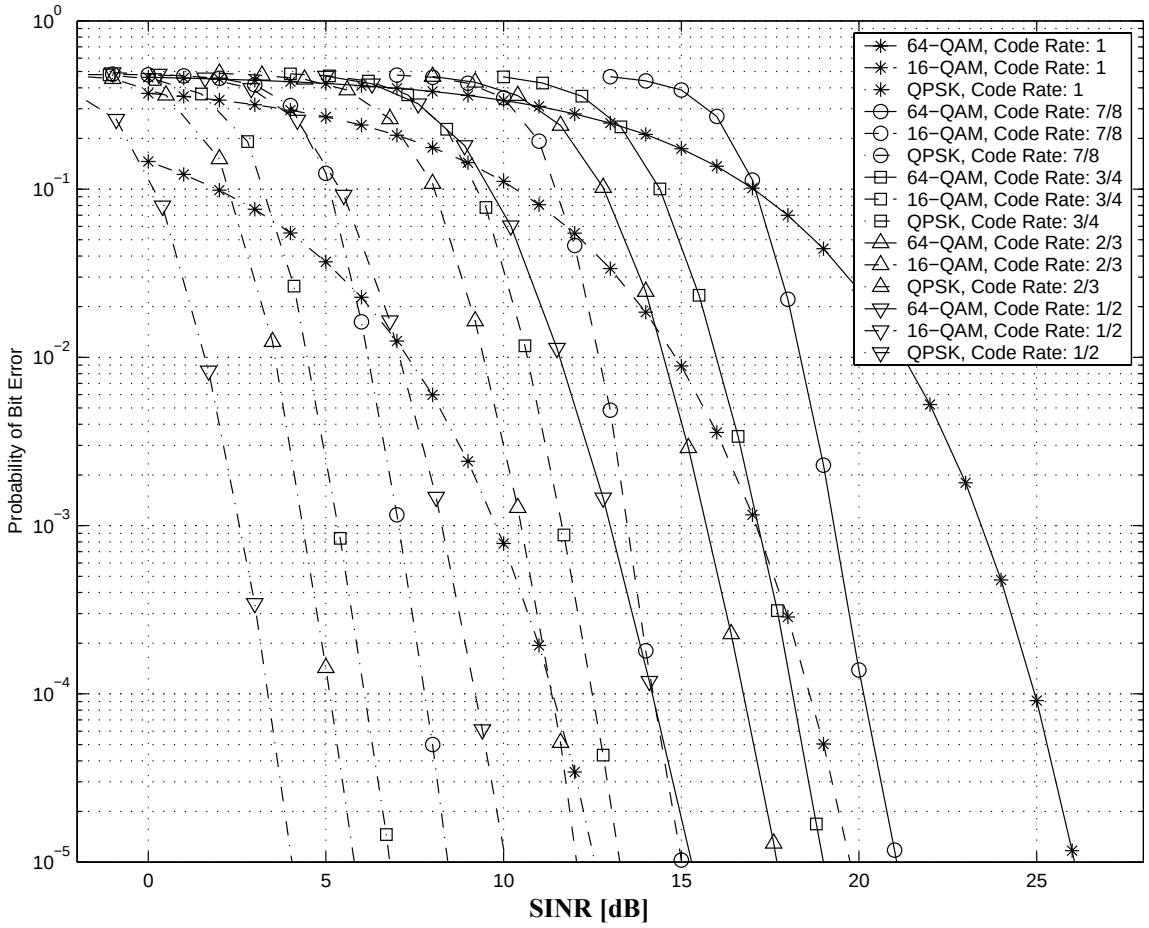

Figure 4: Probability of Bit Error for several combinations of code rates and modulations[1] (assuming the noise plus the interference have Gaussian distribution)

A significant amount of research is conducted on the use of combinations of adaptive modulation and adaptive coding for mobile cellular wireless communication systems. Goeckel [15] investigated the need to use adaptive channel coding considering that the channel condition at the transmission time may be different from the channel condition at the estimation time. He designed adaptive trellis-coded modulation scheme to be employed in a time-varying channel with outdated fading estimates where neither the Doppler frequency nor the exact shape of the auto-correlation function of the channel

[1] These combinations determine the thresholds for adaptive modulation and adaptive coding. Reference: The data used to generate this figure were provided by Dr. Sirikiat Lek Ariyavisitakul, Radia Communications, Norcross, GA, USA

fading process are known. A significant increase in the bandwidth efficiency is found compared with the non-adaptive case.

Muller and Rohling [16] investigated the effect of using channel coding in a system with a narrow-band Rayleigh fading channel. They used a concatenation of Convolutional code and Reed-Solomon code. This combination is shown to have good performance over a large variety of vehicle speeds and demonstrates robustness against Doppler spread.

Lau and Macleod [17] proposed a system model that utilizes variable rate adaptive channel coding for a time-varying flat-fading channel. The system incorporates a low-capacity feedback channel to convey the channel state information to the transmitter. Delay and noise may affect the performance of the feedback channel. According to the channel condition, which is conveyed by the feedback information, the transmitter will select a coding rate so that the received SINR at the receiver meets the requirement according to the current channel condition. The proposed system requires a closed loop scheme to maintain synchronization between the transmitter and the receiver so that the channel condition can be tracked closely. The authors investigated the effect of the delay that is introduced by the feedback channel, the noise on the feedback channel, and the mobile speed.

Goldsmith and Chua [18] combined the coset codes with adaptive M-ary quadrature amplitude modulation (MQAM). Their analytical and simulation results show an effective coding gain of 3-dB compared to an un-coded adaptive MQAM for a simple four-state trellis code, and effective 3.6-dB coding gain for an eight-state trellis code. They also show that more complex trellis codes achieve higher gains.

Ormeci, Liu, Goeckel, and Wesel [19] investigated using adaptive Bit-Interleaved Coded Modulation (BICM). Adaptive BICM schemes remove the need for parallel branches in the trellis, even when adapting the constellation size, thus making these schemes robust to errors made in the estimation of the current channel fading value. The authors use this fact to design adaptive systems that support users with high mobility.

2.4 Power Control

Power control is a technique that controls the transmitted power either at the BS end or the CPE end. Controlling the transmitted power to the minimum required amount for each user, or perhaps with a safety margin, will reduce the co-channel interference that might otherwise be present in a non-power controlled system. Controlling the transmitted power will also prevent a near-to-the-BS user from sending excessive power compared with a far-from-the-BS user, a problem known as near-far problem. Power control can be implemented in the UL direction, the DL direction, or both the UL and the DL direction.

Power control can be implemented in either open loop or closed loop. In open loop power control, the transmitter will determine the required transmitted power based on the quality of the received signal in the opposite direction. For example, when the CPE attempts to access the network through the BS, it transmits signals with a power level that is inversely proportional to the received SINR in the DL direction. If the received SINR, in the DL direction, is very small, that means that the channel conditions are negative; therefore a larger transmitted power is required to be detectable at the BS. Therefore, open loop power control does not require feedback information, which makes it suitable for requesting access to the network without previous knowledge of the channel condition.

Closed loop power control requires feedback information from the receiver to inform the transmitter about the quality of the received signal. Closed loop power control can be further divided into inner loop power control and outer loop power control. Inner loop power control mechanism tracks small-scale variations of the channel, the fading.

Outer loop power control mechanism tracks large-scale variations of the channel, shadowing. Outer loop power control sets the threshold for the inner loop power control to follow.

Figure 5 shows a simplified model for implementing open loop power control in the UL direction.

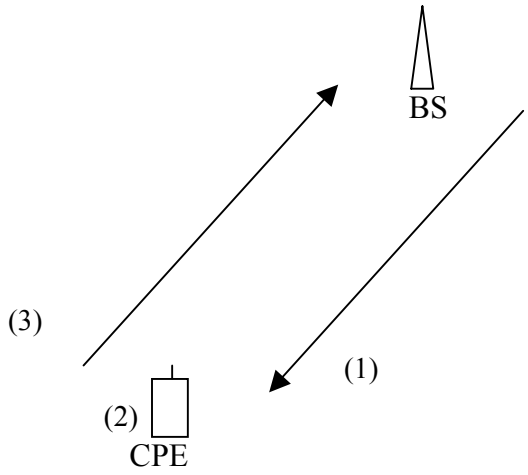

Figure 5: A simplified model for UL open loop power control

The UL open loop power control model can be explained as follows:

1. The CPE measures the received SINR in the DL direction.
2. The CPE evaluates the required transmitted power based on the measured DL-SINR.
3. The CPE transmits the UL channel with the required power.

Figure 6 shows a simplified model for implementing closed loop - inner loop - power control in the UL direction.

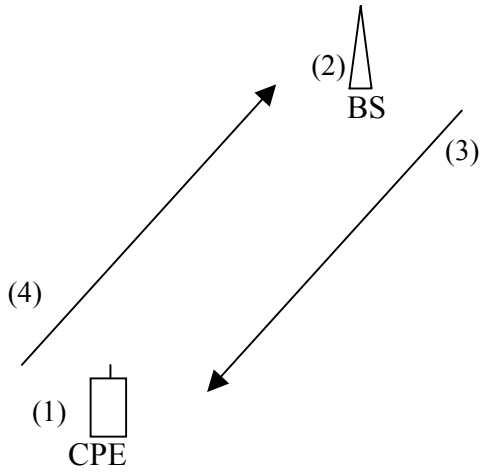

Figure 6: A simplified model for UL closed loop – inner loop - power control

The UL open loop power control model can be explained as follows:

1. The CPE transmits frames in the UL direction.
2. The BS evaluates the received SINR for the UL frame.
3. The BS compares the received SINR with the target SINR, $SINR_{target}$, and transmits feedback information to the CPE, and indicates if the CPE needs to increase the transmitted power, decrease it, or maintain it as in the previous frame.
4. The CPE evaluates the feedback information, updates the transmitted power for the current frame, and sends it in the uplink direction.

Figure 7 shows a simplified model for implementing closed loop - outer loop - power control in the UL direction.

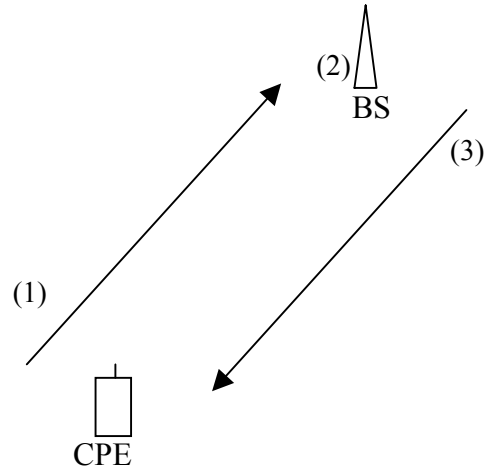

Figure 7: A simplified model for UL closed loop – outer loop - power control

The UL open loop power control model can be explained as follows:

1. The CPE transmits frames in the UL direction.
2. The BS evaluates the received frame error rate, FER, for the UL frames.
3. The BS updates the $SINR_{target}$, based on the measured FER and the target FER, FER_{target}, which is determined by the required Quality of Service (QoS). The $SINR_{target}$ is used in the UL inner loop power control as shown in Figure 6.

Significant research has been conducted on either power control or a combination of adaptive modulation and power control for wireless communication systems. Alouini and Goldsmith [20] studied the capacity of Nakagami multi-path fading (NMF) channels by adapting the transmitted power and the data rate to the channel condition. When the channel condition improves, the system will increase the transmitted data rate and decrease the transmitted power. When the channel condition degrades, the transmitted data rate will be reduced and the transmitted power will be increased. They also considered a system with data rate adaptation and fixed transmitted power. Their results show that optimal power and rate adaptation yields a small increase in capacity over just optimal rate with constant power, and this small increase in capacity diminishes as the average received carrier-to-noise ratio, the Nakagami fading parameter, and/or the diversity branches increase. They also show that the capacity of the Nakagami multipath fading channel is always less than the capacity of the AWGN channel.

Chung and Goldsmith [21] examined adaptive modulation schemes for flat fading channels. Their proposed system adapted the data rate, the transmitted power, and the instantaneous BER with the channel conditions to maximize the spectral efficiency; subject to an average power and BER constraint. They considered continuous and discrete-rate adaptation. They developed a general form for power, BER, and data rate adaptation that maximizes the spectral efficiency for large class of modulation techniques and fading distributions. According to their system model, fixing the transmitted power or the data rate results in minimal loss in the spectral efficiency.

Qiu and Chawla [22] studied the throughput performance gains in third-generation cellular systems that might be achieved by using adaptive modulation and

adaptive coding. Their results indicated that using adaptive modulation alone would result in a significant increase in the throughput compared with SINR balancing power control. Beside the favorable increase in throughput in this case, adaptive modulation will simplify the implementation since it requires fewer measurements compared with any power control scheme. They also found that combining adaptive modulation with a suitable scheme of power control would result in higher throughput than using adaptive modulation or SINR balancing power control alone.

Goldsmith and Chua [23] proposed a variable-rate and variable-power MQAM modulation scheme for high-speed data transmission over fading channels. They derived the spectral efficiency of the MQAM modulation scheme. They showed that there is a constant power gap between the spectral efficiency of the proposed technique and the channel capacity. They also showed that this gap is a simple function of the required BER. By adapting the modulation among six signal constellations, they managed to achieve within 1-2 dB of the maximum efficiency. They computed the rate at which the transmitter needs to update its rate and power in order to keep up with the Doppler frequency. They also estimated the efficiency loss in case the hardware imposes any restriction on the implementation. The authors showed that the combination of adaptive modulation and power control provides power gain of 5-10 dB relative to a power controlled and fixed-rate system and power gain of 20 dB relative to a non-adaptive transmission system. The effect of the channel estimation error and delay on the BER performance is also investigated.

Lau and Maric [24] studied the performance of an adaptive coding scheme in a direct sequence code-division multiple access (CDMA) system that utilizes power

control. They considered both a fast fading channel and a combined fast fading and shadowing channel. The proposed adaptive coding scheme provides significant improvement in the throughput and the BER performance. The study indicated that adaptive coding scheme is relatively robust to shadowing, mobile speed, feedback delay, and finite interleaving depth.

Balachandran, Kadaba, and Nanda [25] proposed a technique to estimate the channel quality for a cellular mobile radio communication system that utilizes a set of coded modulation schemes and power control. They mapped the average Euclidean distance (ED) to the SINR per symbol. The measured SINR is used to measure the channel quality. The authors showed that the proposed Euclidean distance metric works well across the entire range of Dopplers to provide a near-optimal rate adaptation performance. The proposed method of adaptation averages out short-term variations due to Rayleigh fading and adapts to the long-term variations due to shadowing. At low Doppler frequencies, the Euclidean distance metric can track Rayleigh fading and shadowing, which will further increase the throughput.

Chapter 3: Thesis Problem and System Model

3.1 Introduction

In this chapter, we state the thesis problem under investigation. We next describe the system model that is used to analyze the proposed solution.

3.2 Thesis Problem to be Investigated

Almost all of the previous works that investigated the advantage of using adaptive techniques for cellular wireless systems were geared towards mobile systems with voice applications, i.e. relatively low data rate. In this thesis, we will investigate the advantages of using these techniques for broadband fixed cellular wireless communication systems with applications that require high data rates.

In a typical broadband wireless cellular system, the base station (BS) will transmit to all customer premises equipments (CPEs) in the downlink direction; the CPEs will communicate back to the BS in the uplink direction. The services that might be offered in this system – Internet, video, audio – suggest that the downlink traffic will likely be larger, if not much larger, than the uplink traffic. Therefore, our research will focus on improving the performance of the downlink direction of the system.

Adaptive modulation, channel coding, and power control are well-known techniques that are utilized in mobile cellular wireless communication systems. These techniques have shown a significant improvement in the performance of mobile networks as shown in chapter 2. Our research will apply several combinations of these techniques to broadband fixed cellular wireless communication systems.

The performance metric that will be used to evaluate the system performance is the throughput measured as the effective average modulation efficiency, which is defined as the average received information-bits/sec/Hz. For example, if the BS chooses 16QAM without coding to match the current channel condition in the DL direction, and assuming that the information is received correctly at the CPE, then the effective modulation efficiency is 4 information-bits/sec in one Hz of the transmission bandwidth; i.e. 4 information-bits/sec/Hz. Channel coding may be combined with adaptive modulation to improve the throughput. The coding scheme is Bit Interleaved Coded Modulation (BICM) with several code rates, as shown in chapter 2. If the BS selects a combination of 16QAM and BICM with code rate 1/2, and assuming that the information is received correctly at the CPE, then the effective modulation efficiency is 2 information-bits/sec in one Hz of the transmission bandwidth, i.e. 2 information-bits/sec/Hz. In our simulations, we transmit 100,000 times in the DL direction, and then we take the average of the effective modulation efficiency over the N transmissions, which provide the effective average modulation efficiency.

Table 1 illustrates our approach for investigating the advantage of using the adaptive techniques in broadband fixed wireless communication systems. Two systems are used for the evaluation process, as shown in section 3.3: system type 1 and system type 2. In the first case, the throughputs of three systems, of type 1, using fixed modulation: QPSK, 16QAM, or 64QAM are compared with the throughput of another system, also type 1, utilizing adaptive modulation, i.e. combinations of QPSK, 16QAM, and 64QAM. In case 2, system type 1, utilizing adaptive modulation is compared with another system, also system type 1, using a combination of adaptive modulation and

adaptive coding. In case 3, system type 2 is used to compare the throughput of a system utilizing adaptive modulation with another system that uses a combination of adaptive modulation and power control. In case 4, the throughput of fixed modulation is compared with those of adaptive modulation, the combination of adaptive modulation and adaptive coding, the combination of adaptive modulation and power control, and the combination of adaptive modulation, adaptive coding and power control. This case will show the impact of each technique, or combination of techniques on the throughput of the system and, therefore, provide some design guidelines for the optimum use of these techniques.

		Compared Techniques				
System type 1	Case 1	FM	AM			
	Case 2		AM	AM + AC		
System type 2	Case 3		AM		AM + PC	
	Case 4	FM	AM	AM + AC	AM + PC	AM + AC + PC

Table 1: Investigated adaptive techniques

Legend:
FM: Fixed Modulation
AM: Adaptive Modulation
AC: Adaptive Coding
PC: Power Control

3.3 The System Model

Several issues related to modeling the system are investigated in the literature. We start with a review of some these issues, and then we present our system model.

M. Turkboylari and G. L. Stuber [26] proposed an algorithm for estimating the signal-to-interference-plus-noise ratio (SINR) in TDMA cellular systems. They evaluated the algorithm for use in the IS-54/136 and a GSM-like system, and compared it with the existing techniques. The authors found that the algorithm has a mean square prediction error that is comparable to the best-known SINR estimation schemes, but with a significantly reduced computational complexity.

Falconer, Adachi, and Gudmundson [27] presented an overview for time-division multiple-access (TDMA). The authors summarized a number of frequency and timeslot allocation techniques for enhancing the capacity and flexibility of TDMA-based systems. The problems of fading, delay spread, time variability, and interference are explained in the context of TDMA systems. They show how these problems can be countered, using appropriate techniques of detection, diversity, coding, adaptive equalization, and slow frequency hopping.

Gray [28] presented an overview for a broadband local access system at 28 GHz, including the FCC band-plan. The author proposed a utilization plan for the spectrum. The architecture of the Local Multipoint Distribution Service (LMDS) is described along with link budgets and capacity estimates. The author provided an overview concerning the advantages and disadvantages of the LMDS systems at 28 GHz.

Woerner, Reed, and Rappaport [29] identified key simulation issues for mobile wireless cellular systems. These issues address several design challenges that stem from

the mobility of users throughout the system, the time-varying Multipath channel, and the interference. Computer simulations are used in cases where the complexity and the time-varying nature of the mobile radio channels and systems cannot be fully represented by analytical techniques. They presented some examples for link-level and system-level performance issues that can be addressed in a simulation environment.

Kajiwara [30] investigated the attenuation characteristics of foliage at 29.5 and 5 GHz for Local Multipoint Distribution Services (LMDS). The author demonstrates that the attenuation level in dB could be modeled as Rician distribution. The Rician parameter depends on the leaf size, the total area of leaves and the humidity in climate. Accordingly, swaying foliage in wind causes a significant channel fading at 29.5 GHz, ranging over 10dB, and the fading depth at 5GHz is approximately 2dB. The smaller diffraction loss through leaves is attributed to the smaller fading depth at 5 GHz compared with the fading at 29.5 GHz. The author also shows that polarization diversity gain is difficult to achieve in LMDS channel, obstructed by foliage because of a relatively strong correlation.

Yip and Ng [31] developed a discrete-time model for digital communications via a frequency-selective Rician fading, wide-sense-stationary uncorrelated-scattering (WSSUS) channel with arbitrary pulse shaping and receiver filtering. The model also applies to a frequency-selective Rayleigh fading WSSUS channel. The authors derived statistical characteristics for the complex-valued noise due to AWGN, N_k, and the time-varying attenuation that is introduced by the channel, $g_m(t)$. Simple closed-form formulas computing statistical parameters of N_k and $g_m(t)$ are also derived.

Hansen and Meno [32] derived a closed form solution for the probability

distribution of the received power for a channel that has Rayleigh fading distribution and lognormal shadowing superimposed on the Rayleigh fading part. The authors illustrate the proposed solution.

Gong and Falconer [33] studied the effect of a number of factors on the performance of Local Multipoint Communication Services (LMCS) at 28 GHz frequency band. The myriad factors include beamwidth and gain ratio of directional antennas, sectorization of hub antennas, propagation exponent, lognormal shadowing, site diversity, and transmitter power control. The authors considered line-of-site (LOS) and non-line-of-site (NLOS) system models. They illustrate that highly directional antennas at the subscriber side could dramatically improve the system performance for both the uplink and the downlink direction. They also argued that an outage probability of 0.9% could be achieved for a NLOS system whereas a LOS provides an outage probability of as low as 0.3%.

Rappaport and Fung [34] employ a statistical Multipath channel simulator to evaluate the performance of FSK, BPSK, and $\pi/4$ QPSK. They also present in [35] a combination of hardware and software simulation tool that is used to simulate the bit error rate for $\pi/4$ DQPSK mobile radio communication systems with a channel that is characterized by a two-ray model.

The simulation is based on two system models: system type 1 and system type 2. System type 2 is an elaborate version of system type 1. System type 1 is presented first. System type 1, as shown in Figure 8, consists of a grid of 3 cells by 3 cells. Each cell is divided into 4 sectors. Each sector is square in shape with side length of 2000 m. Perfect frequency polarization reuse is utilized in each sector, which allows each sector to use the

entire bandwidth without suffering from adjacent channel interference. The user of interest is located in sector # 10. All sectors that use the same frequency band and same frequency polarization as sector # 10 are shadowed in Figure 8. Each cell is served by a 4-sectored antenna, with a beamwidth of 90^o for each sector, resulting in a 90^o beamwidth antenna for each sector. System type 1 is used to evaluate cases 1 and 2 as shown in Table 1.

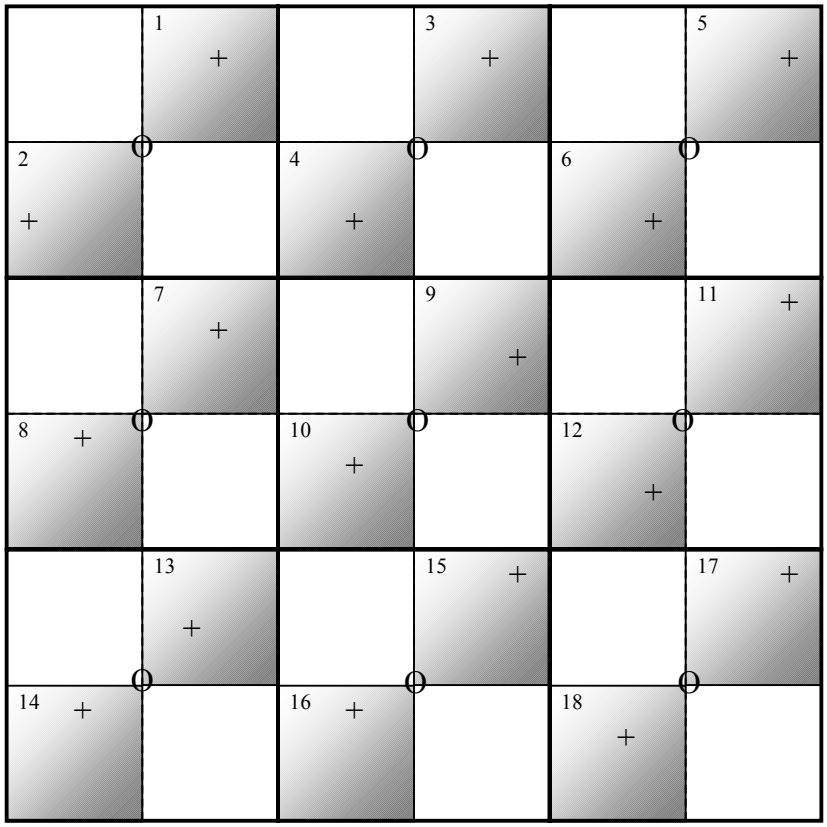

Figure 8: System type 1 layout

Where:

⊗ : A back-to-back 90-degrees beamwidth antenna.

+: A randomly located CPE.

System type 2 uses system type 1 as a building block, where system type 1 is

organized as a grid of 3 by 3 as shown in Figure 9. System type 2 is used to evaluate two cases, 3 and 4, where power control is involved. In these cases, all *BS*s start transmitting using the maximum possible transmitted power in order to maximize the throughput. Then each BS will reduce its transmitted power, according to the feedback from the CPE, to meet the current required SINR plus 10% safety margin. When every BS in the network reduces its transmitted power, the interference on the CPE will decrease and consequently, its SINR will increase, which will result in either increasing the throughput or reducing its own transmitted power. This protocol will result in maximizing the throughput for all the users in the network while reducing the transmitted power and the interference.

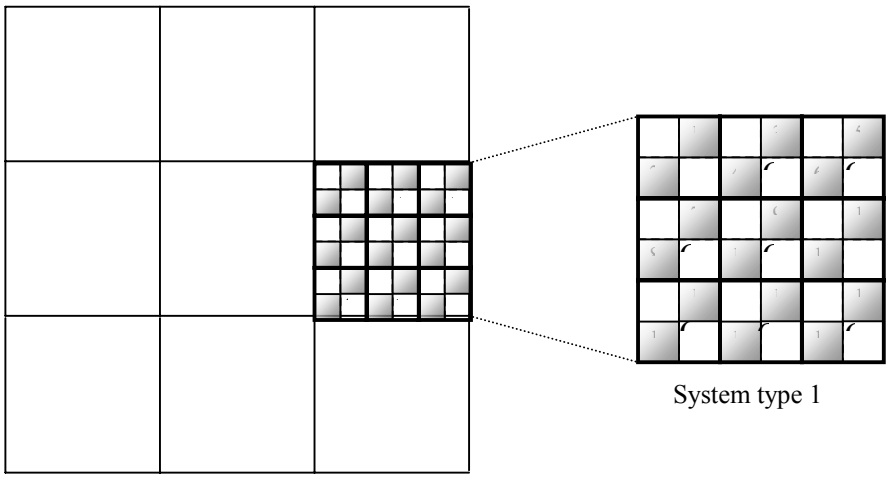

Figure 9: System Type 1 as a building block of system type 2

Since the downlink direction is considered in the research, the base stations of all sectors that have common frequency polarization with the user of interest, which is located in sector # 10, represent interferers for the user of interest. In other words, there are 17 interferers for the user of interest in addition to the thermal noise.

We assume that all base stations and all users use ideal antenna, as shown in Figure 10. Part (a) of this figure illustrates the details of the base station's antenna where the main lobe beam width is 90^o and the main lobe and the side lobe gains are G_m and G_s respectively. Part (b) of the same figure illustrates the details of the user equipment's antenna. The user equipment's antenna is quite similar to the base station's antenna, with the exception of the beam width of the main lobe, 2β [degrees], which is used as an evaluation parameter in the simulations, as will be shown in chapter 4.

We assume that only one user equipment is operating in each sector. Therefore, adjacent channel interference is not taken into account in our simulation. Furthermore, each user utilizes the entire bandwidth in each sector. The user of interest, and all the

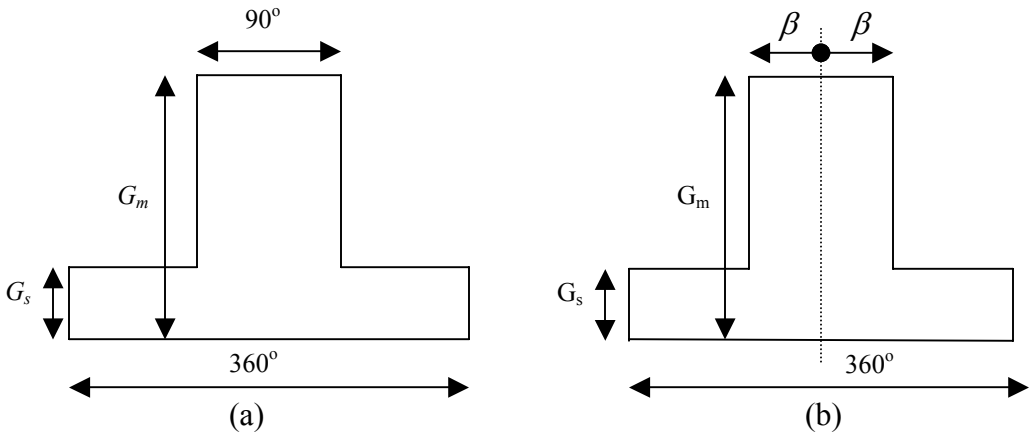

Figure 10: The antenna beam widths and gains for (a) the base station and (b) the user equipment

corresponding interferers are located randomly, and distributed uniformly, in each sector. Therefore, care must be taken in order to ascertain whether the main lobe gain or the side lobe gain of the antenna is used in calculating the received power of the user's signal and the interferences' signal at the CPE. Calculating the value of the antenna gain,

at the CPE, is an elaborate process and should be considered for each base station.

Figure 11 shows the antenna gain model with emphasis on the angle of arrival, α, from the BS transmitter to the centre of CPE's antenna. α is calculated as follows:

$\alpha = \phi - \theta$, where ϕ and θ are defined and calculated as shown below.

Figure 12 shows the method of calculating the angle of arrival, α, from BS # 3, which serves sectors # 5 and # 6, to the CPE of the user of interest, which is located in sector # 10. The angles ϕ and θ are defined as follows:

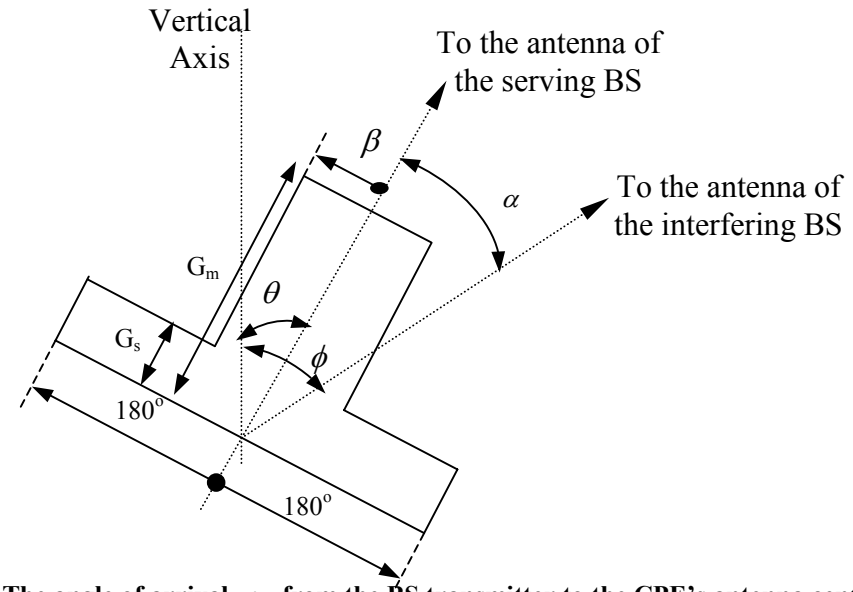

Figure 11: The angle of arrival, α, from the BS transmitter to the CPE's antenna centre

ϕ : The angle, toward the CPE, of a right-angled triangle that is formed by BS # 3 and the CPE as two edges of the hypotenuse. ϕ is calculated as follows:

$$\phi = \tan^{-1}\left(\frac{2 \times \sec tor\_length + a}{2 \times \sec tor\_length + b}\right)$$

θ : The angle, toward the CPE, of a right-angled triangle that is formed by the serving BS, BS # 5, and the CPE as two edges of the hypotenuse. θ is calculated as

follows:

$$\theta = \tan^{-1}\left(\frac{a}{b}\right)$$

To keep the calculations as simple as possible, the gain of the CPE's antenna, i.e. the gain of the receiving antenna, $G_{r,}$ is calculated as follows:

If $\alpha \leq \beta$, the main lobe gain of the CPE's antenna is used as G_r to calculate the received signal power.

Else if $\alpha > \beta$, the side lobe gain of the CPE's antenna is used as G_r to calculate the received signal power.

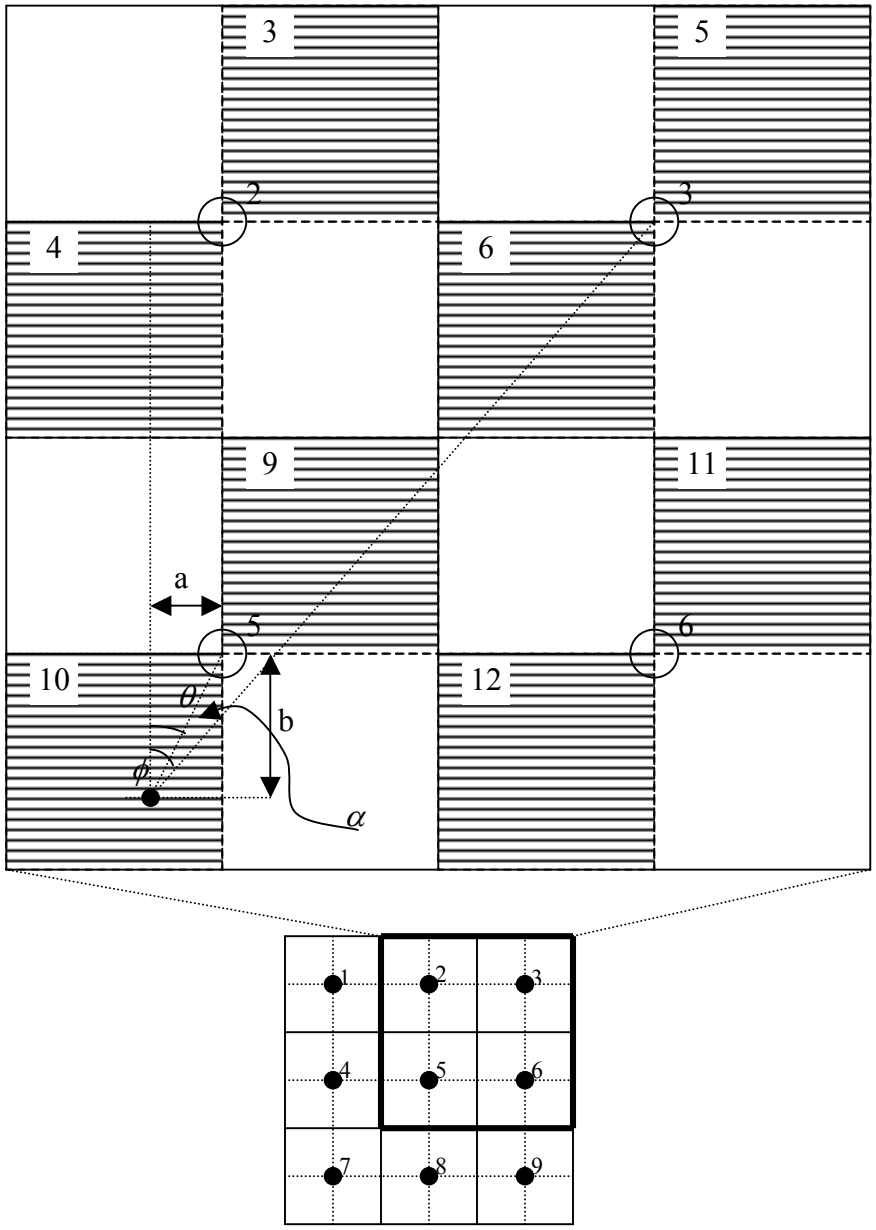

Figure 12: Evaluating the angle of arrival, α , at the CPE's antenna

We propose a system model with similarities to the model that Fung [35] used to evaluate the $\pi/4$ DQPSK system. The system model is shown in Figure 13, where the data is modulated by the suitable modulation scheme and then transmitted over Rician fading channel. AWGN is added to the result and then interference is added. The received SINR is calculated at the CPE side.

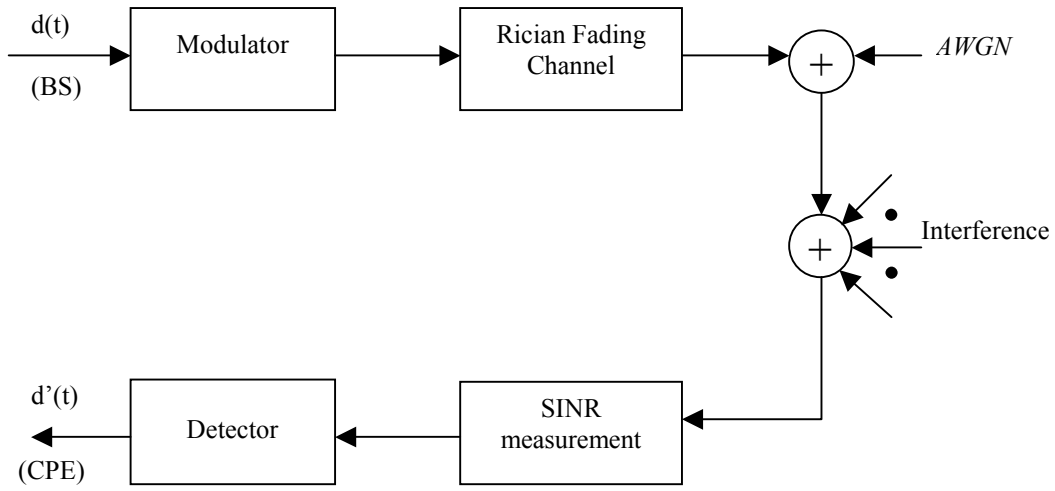

Figure 13: The proposed system model

The received signal strength, in the DL direction, is calculated as follows:

$$P_r[dBm] = P_t[dBm] + G_t[dB] + G_r[dB] - \left(20\log\left(\frac{2\pi d_o f}{c}\right)[dB] + 10n \times \log\left(\frac{d}{d_o}\right)[dB] \right) + X_\sigma[dB] + F[dB]$$

Where:

P_r = the received signal power at the CPE's antenna, in dBm.

P_t = the transmitted signal power from the BS, of the serving antenna or the interfering antenna, in dBm.

G_r = the transmitting antenna gain, in dB.

G_r = the receiving antenna gain, in dB.

d_o = the reference distance, in meters. d_o is assumed to be 50 m is this research.

f = the operating frequency, in Hz.

c = the speed of light, 3×10^8 m/sec.

n = the propagation exponent for the path loss.

d = the distance of the user from the BS. This distance can be easily calculated from the geometry of the cellular system, as shown in Figure 12.

X_σ = A random variable, normally distributed in dB, that accounts for the large-scale variations of the channel, i.e. shadowing.

F = A random variable that accounts for the small-scale variations, i.e. the fading, of the channel, in dB. The Rician fading channel model is used in this research. The Rician parameter is generated as follows [11]: Let K be the Rician parameter, then A and B are as follows:

$$A = \sqrt{\frac{2K}{2K+2}},$$

$$B = \sqrt{\frac{1}{2K+2}},$$

Furthermore, let x and y be normally distributed random numbers, with standard deviation of 1 (this value of the standard deviation will result in an average power of 1 due to the Rician fading channel), then

$a = B \times x$ and

$b = B \times y$. A Rician distributed signal is given by

$Rician\_Signal = \sqrt{(a + A)^2 + b^2}$, and F is given by

$F[dB] = 10\log_{10}[(a + A)^2 + b^2]$

The thermal noise is considered for the calculations of the received signal-to-interference-plus-noise ratio, SINR, as follows [12]:

$N = N_o \times W$ [m watts]

$N_o = \kappa \times T^o$ [m watts/Hz]

$\kappa = 1.38 \times 10^{-23}$ *W*/K-Hz = ─228.6 dBW/K-Hz.

$T^o = 290$ [Kelvin]

W = the transmission bandwidth, in Hz.

Where:

N: is the thermal noise in milli-watts or dBm

N_o: is the single-sided thermal noise power spectral density in milli-watts/Hz

κ : Boltzmann's constant

T^o: is the temperature in Kelvin

A noise figure, *F*, of 8 dB will be added to the noise to account for any noise that is added by the network. Therefore the total thermal noise, N_T, is given as follows:

N_T [dBm] = *N* [dBm] + *F* [dB]

A fully loaded system is considered where one user is randomly located in each sector and all the base stations, the serving and the interfering base stations, are transmitting in the DL direction. In order to improve the efficiency, we propose a frame structure as shown in Figure 14. Each frame starts by a training sequence (TS) followed by signaling period (SP) and then a series of packets for all the users in the sector. The BS will start by transmitting the TS to all users in the sector. The user of interest will calculate the received signal power, *S*, the sum of all of the received interference powers, *I*, and the thermal noise, N_T. It will then calculate the received signal-to-interference-plus-noise ratio, SINR as follows:

$$SINR = \frac{S}{I + N_T}$$

This value is used in the water fall-like curves, in the adaptive modulation case or the combination of adaptive modulation and adaptive coding case, to find the appropriate constellation size, or the combination of constellation size and coding rate that will meet the required BER, as shown in chapter 2. The CPE will send this information to the BS over an error-free feedback link that is provided by a FDD scheme. The BS will then use this information to send the current frame using the current combination of constellation size and code rate. The channel is assumed constant over one frame. This assumption will allow the BS to transmit the current packet, or group of packets, using the current feedback information from each CPE.

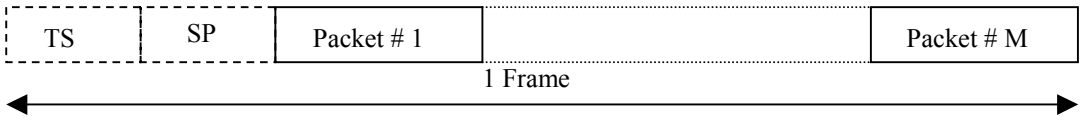

Figure 14: The frame structure for the DL transmission

From the constellation size, or the combination of the constellation size and code rate, the received number of information bits/sec in each Hz of the transmission bandwidth can be calculated. In our simulation, 100000 transmissions are made in the DL direction according to the aforementioned scheme. The average over 100000 transmissions will give the effective average modulation efficiency of the examined technique; i.e. the throughput.

When power control is combined with adaptive modulation, or adaptive modulation and adaptive coding, The BS will send a training sequence to the CPE. The CPE will evaluate the received SINR and will send feedback information to the BS informing it about the nearest lower constellation size (refer to Figure 1 in Chapter 1). The BS will reduce the transmitted power to meet the requirement of the selected constellation size plus 10% safety margin. All base stations in the system will follow the same approach for controlling the transmitted power. A delay-free and error-free feedback link is assumed to be present from the CPE to the BS.

Chapter 4: Simulation Results, Part 1

4.1 Introduction

In this chapter, we present the simulation results for the system modeled in the previous chapter. The objective of these simulations is to determine the improvement in the throughput of the system by modifying several parameters. The remaining sections of this chapter demonstrate the advantage of using adaptive modulation.

Several performance metrics are used to investigate the advantage of using adaptive modulation for broadband fixed wireless systems. Figure 15 shows the metrics that will be explained in detail in this chapter. Each block in this figure illustrates the independent parameter and the metric that are used. It also states whether this metric is applied to a subset of users or to all the users. Throughout this chapter, the user of interest is placed at several distances along the diagonal of the sector. This positioning scheme may not have a significant difference, from a random positioning scheme, on the throughput of the system since this positioning scheme may affect the receiving gain of some of the interferers. All the interferers are placed randomly in their sectors. Furthermore, for each case we consider the performance at three positions from the base station. The first position is at 50 m from the BS (this position is affected by the free space propagation model). The second and the third positions, at 1400 m and 2800 m respectively, are affected by a propagation exponent of 4.

Chapter 5 examines the advantage of combining adaptive coding and power control with adaptive modulation. The same chapter concludes with statistical results that provide an insight into the system performance.

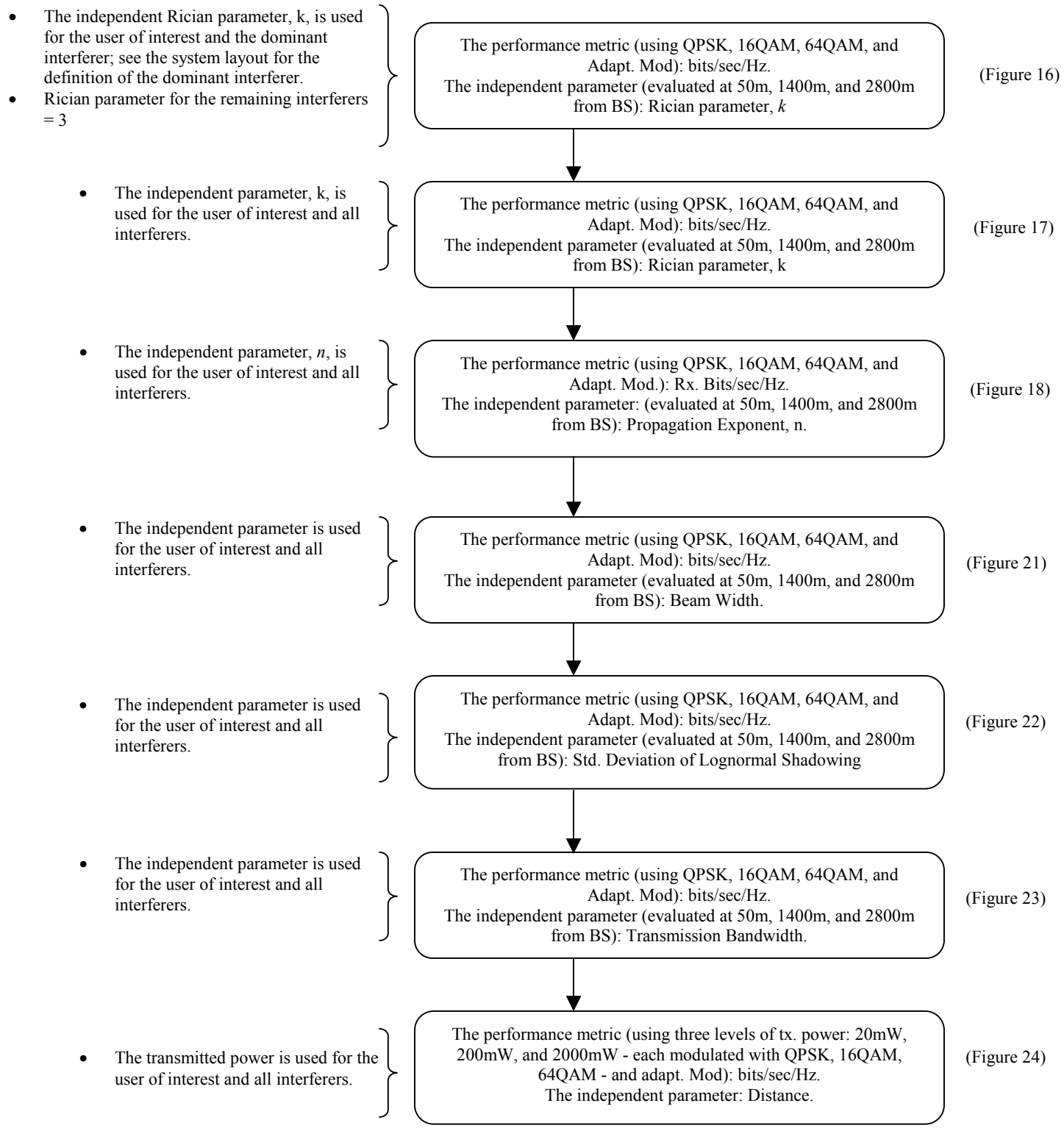

Figure 15: The impact of various parameters on the system performance (the throughput)

4.2 Rician Parameter

The effect of Rician parameter, *k*, on the system throughput is investigated in two different approaches: The first approach is explained in subsection 4.2.1 and the second approach is explained in subsection 4.2.2.

4.2.1 Rician Parameter for the user of interest and the dominant interferer

In the first approach, one *k* value is employed for the user of interest and the dominant interferer, while *k* for the remaining interferers is set to 3. Adaptive modulation is used without error control coding or power control. The simulation is considered for three locations, near the base station, near the middle of the sector, and near the edge of the sector, as shown in Figure 16. The results are classified according to the user's location from the base station as follows:

Near the base station: The results show that the throughput does not increase significantly with *k*. This is a high SINR scenario. The results also show that adaptive modulation outperforms any single modulation regardless of *k* value. Adaptive modulation improves the throughput, by about 1.2 info bits/sec/Hz, compared to the best performing modulation scheme. All the results will be labeled as info bits/sec/Hz rather than bits/sec/Hz, even in cases where no error control coding is used, to give a common metric for comparing the results.

The effective average modulation efficiency never reaches the maximum value for any fixed modulation case. For example, the effective average modulation efficiency levels off at 1.75 info bits/sec/Hz for QPSK. This is due to the presence of the noise and the interference (dominated by the dominant interference), which results in the received signal being below the acceptable threshold for about 12.5% of the total transmission

time. This will result in effective average modulation efficiency of 1.75 info bits/sec/Hz.

For the effective average modulation efficiency of the adaptive modulation case, the receiver selects the largest possible threshold, starting from 6 bits (for 64-QAM) then 4 bits (for 16-QAM) and ends with 2 bits (for QPSK). If the received SINR doesn't match any of these thresholds, then no bits (0) will be received. Averaging over all the transmissions, at each position, will result in a point in the adaptive modulation curve. For example, the effective average modulation efficiency when k equals 1 is 4 info bits/sec/Hz.

Near the middle of the sector: Increasing k from 0 to 4 will improve the throughput for 16-QAM, 64-QAM and adaptive modulation. The performance of QPSK will improve in the vicinity of k equal to 0 to 2. The throughput will not be affected if k is larger than 6 at this location. The results also show that adaptive modulation has better performance than any single modulation regardless of the value of k. The performance improvement is about 0.4 info bits/sec/Hz when k equals 0, the improvement increases to about 0.7 info bits/sec/Hz when k is larger than 6.

Near the edge of the sector (noise limited scenario): The results show that increasing k from 0 to 2 improves the performance for QPSK and 16-QAM. The throughput for 64-QAM and adaptive modulation increases when k increases from 0 to 8. Increasing k above 8 will have no impact on the throughput. Adaptive modulation improves the performance, regardless of the value of k. The improvement varies from 0.02 info bits/sec/Hz when k is 0 to 0.06 info bits/sec/Hz, when k is larger than 8.

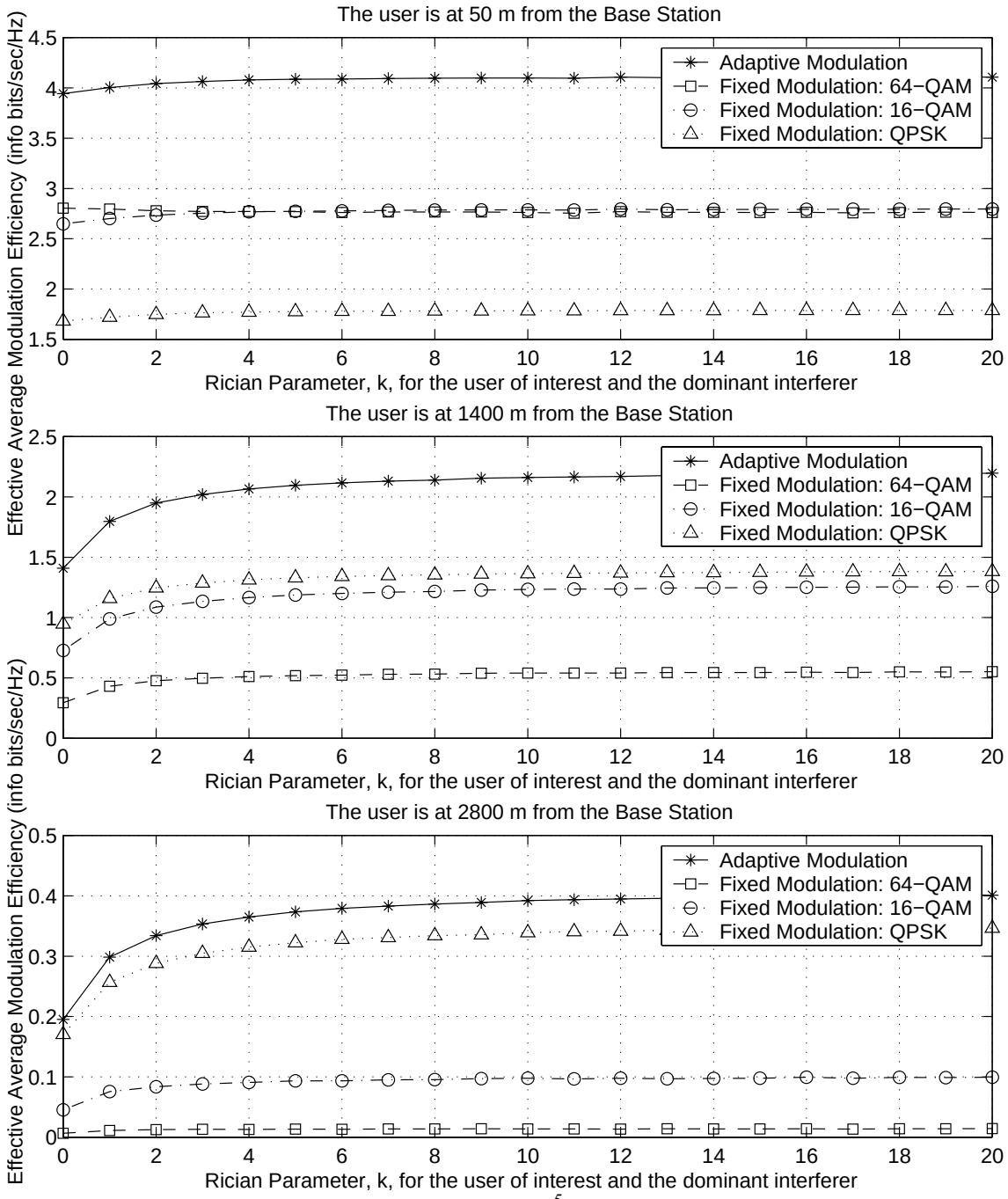

[Downlink transmission, f_c =2.5 GHz, BER =10^{-5}, T_x BW =6 MHz, T_x Power =200 mW, Propagation exponent for the user and all the interferers =4, Std. Dev. of log normal shadowing =7 dB, Antenna beam width for the BS=90^o, Antenna beam width for the user and all the interferers =30^o, Antenna gains for the B.S, the user of interest, and all the interferers: Main lobe =15 dB, Side lobes =-10 dB]

Figure 16: The impact of Rician Parameter (for the user of interest and the dominant interferer), *k*, on the system performance. *k* = 3 (for the remaining interferers)

4.2.2 Rician Parameter for the user of interest and all the interferers

In the second approach, the user of interest and all the interferers are assumed to have the same k value. Adaptive modulation is used without error control coding or power control. The performance is considered at three locations: near the base station, near the middle of the sector and near the edge of the sector, as shown in Figure 17.

Near the Base station: An improvement in the throughput is obtained when k increases from 0 to 2 for QPSK, 16-QAM, and adaptive modulation. Increasing k above 2 does not improve the throughput. That is because the throughput at this location is limited by the dominant interferer. Adaptive modulation improves the performance, compared with any single modulation, regardless of the value of k.

Near the middle of the sector: Increasing k from 0 to 2 will increase the throughput for QPSK. The throughput for 16-QAM, 64-QAM, and adaptive modulation will increase when k increases from 0 to 6. Increasing k above 6 will have little impact on the throughput. Adaptive modulation increases the throughput, compared with any single modulation, regardless of the value of k.

Near the edge of the sector: Increasing k from 0 to 1 will have a minimal impact on the throughput for QPSK. When k increases from 0 to 4, the throughput for 16-QAM will increase. 64-QAM and adaptive modulation show improvement in the throughput when k increases from 0 to 10. Increasing k above these limits will have no impact on the throughput.

Comparing section 4.2.1, k for the user of interest and the dominant interferer as a performance metric, and section 4.2.2, k for the user of interest and all the interferers as a performance metric, we notice that the system has similar performance in both cases. In

other words, varying k for the interferers will have little impact on the system performance. The reason for this observation is because the transmitted power of the interferers, being located far from the user of interest, undergoes a large amount of path loss, with a propagation of exponent equal to 4. The received power from the interferers, with the exception of the dominant interferer, is minimal even if the line-of-sight component is large compared to the reflected paths; i.e. k is large.

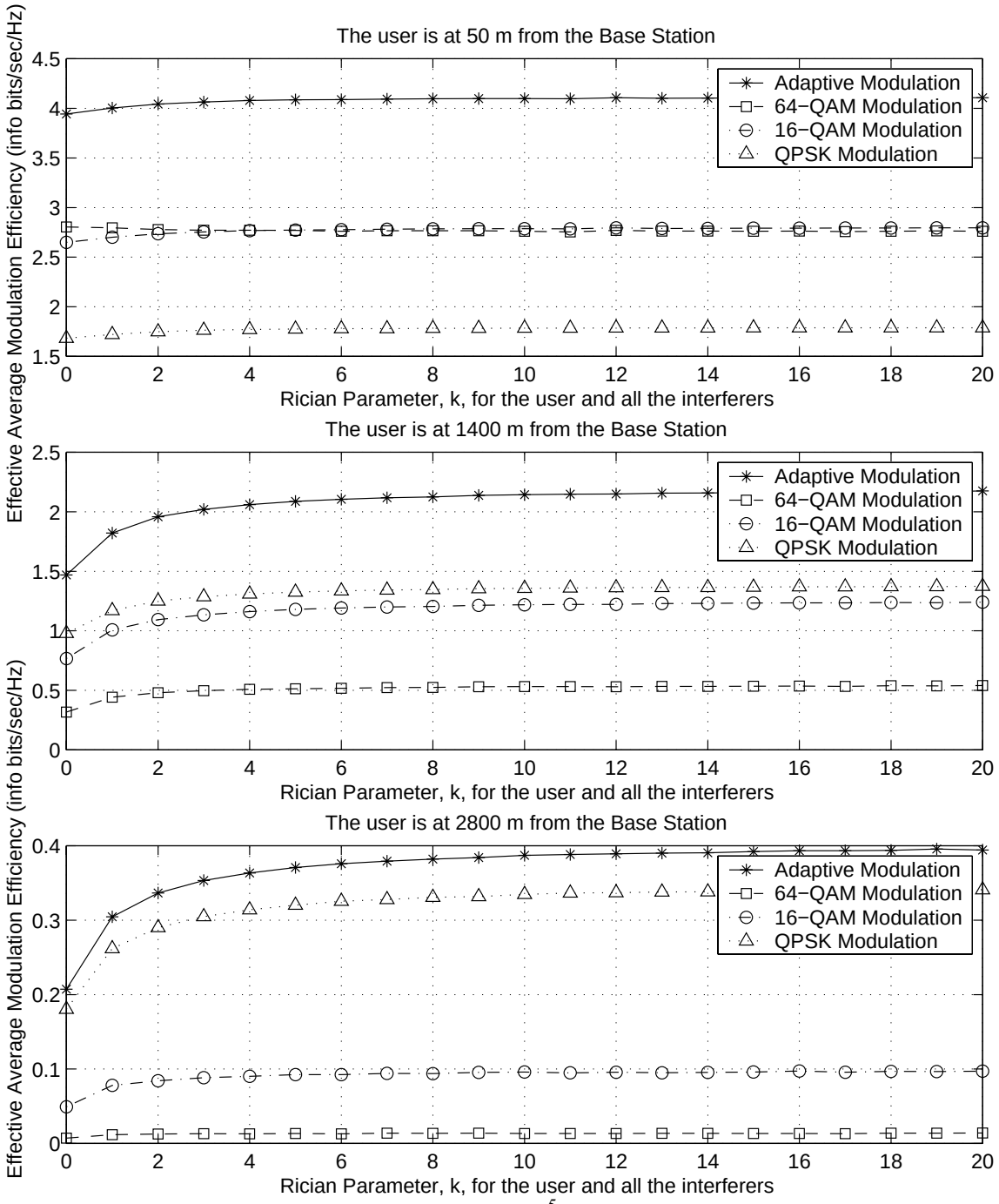

[Downlink transmission, f_c =2.5 GHz, BER =10^{-5}, T_x BW =6 MHz, T_x Power =200 mW, Propagation exponent for the user and all the interferers =4, Std. Dev. of log normal shadowing =7 dB, Antenna beam width for the BS=90^o, Antenna beam width for the user and all the interferers =30^o, Antenna gains for the B.S, the user of interest, and all the interferers: Main lobe =15 dB, Side lobes =-10 dB]

Figure 17: The impact of *k* value (common for the user of interest and all interferers), *k*, on the system performance.

4.3 Propagation Exponent

The impact of the propagation exponent, *n*, on the system throughput is examined in this section. It is assumed that the user of interest and all interferers have the same propagation exponent. Adaptive modulation is used without error control coding or power control. The performance is considered at three locations: near the base station, near the middle of the sector and near the edge of the sector (noise-limited), as shown in Figure 18. The results are classified according to the user's location from the base station as follows:

Near the base station: increasing *n* has little effect on the throughput in this high SINR scenario. Using adaptive modulation significantly improves the performance near the base station regardless of the value of the propagation exponent.

Near the middle of the sector: Increasing *n* from 2 to 3.5 will result in a linear increase in the throughput for all single modulations as well as for adaptive modulation. This increase is due to the fact that increasing *n* within this region will increase the path loss for the interferers more than increasing the path loss for the user of interest. In other words, increasing *n* between 2 and 3.5 will reduce the received interference power more than reducing the received signal power. Therefore, the received SINR at the user of interest will increase with increasing *n* from 2 to 3.5. The situation reverses when *n* is in the region between 3.5 and 5.75. In this region the system is noise limited and, therefore, increasing the propagation exponent will reduce the received signal strength for the user of interest while the thermal noise is fixed. Therefore, the received SINR will decrease with the increase of *n* from 3.5 to 5.75. If *n* increases above 5.75, the received signal will decrease sharply so that the received SINR will not meet the requirement for any single

modulation nor the adaptive modulation case. Therefore, the throughput will be zero in this region. Adaptive modulation will increase the throughput compared with any single level modulation.

Near the edge of the cell: The performance at this location has a similar, but contracted, shape as that of the performance near the middle of the sector. The performance has reduced at this location because the received signal to the user of interest decreases due to increasing the path loss. Therefore, the received SINR is generally smaller than the previous two cases.

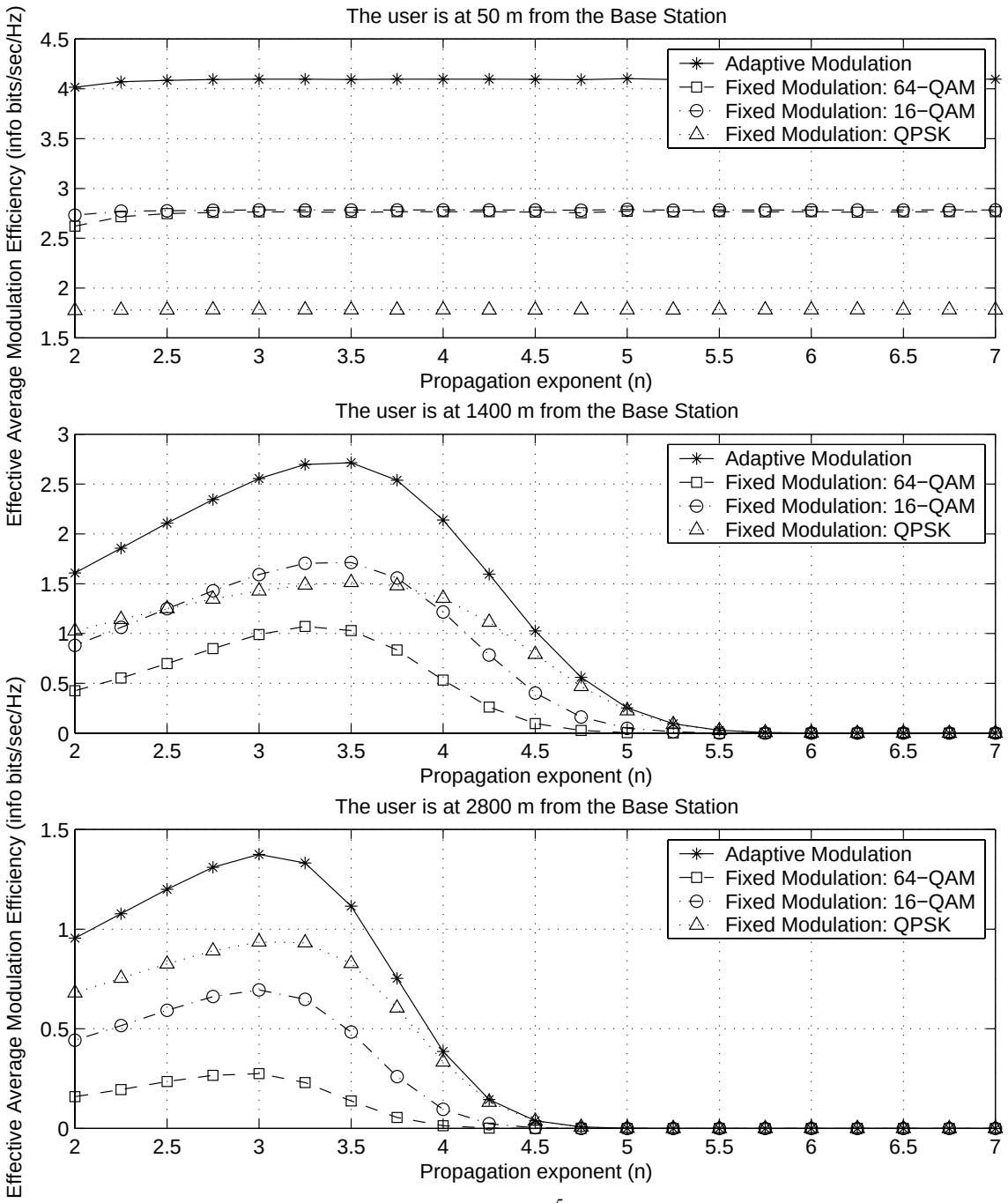

[Downlink transmission, f_c =2.5 GHz, BER =10^{-5}, T_x BW =6 MHz, T_x Power =200 mW, Rician parameter for the user of interest and the dominant interferer= 8, Rician parameter for the remaining interferes =3, Std. Dev. of log normal shadowing =7 dB, Antenna beam width for the BS=90^o, Antenna beam width for the user and all the interferers =30^o, Antenna gains for the B.S, the user of interest, and all the interferers: Main lobe =15 dB, Side lobes =-10 dB]

Figure 18: The impact of the propagation exponent, *n*, on the system performance

4.4 Beam Width

Reference [37] shows that reducing the antenna beamwidth will reduce the interference that is collected in the antenna main lobe. Reducing the interference will reduce the probability of outage in the system.

The impact of the beam width of the user of interest, θ, on the system throughput is investigated in this section. Fixed modulation and adaptive modulation are used without error control coding or power control. The base station utilizes a sectored antenna with a beam width of 90^o. The antenna gain is closely related to its beam width as shown in reference [36]. Reducing the antenna beam width of the user of interest will increase its gain. We assume that the antenna is ideal, with a main lobe beam width of 2θ as shown in Figure 19.

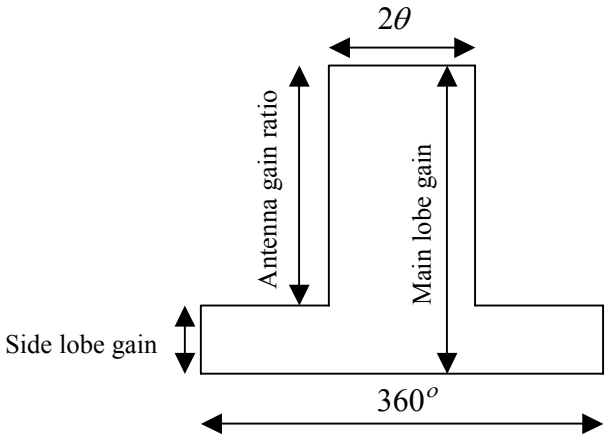

Figure 19: The gains of an ideal antenna

Reference [36] shows that the gain of the main lobe for the antenna is expressed in dB as follows:

$$G_{main\_lobe} = 10\log\frac{1}{\sin^2(\theta/2)}[dB]$$

Figure 20 shows the relationship between the antenna beam width and the main lobe gain. As the antenna beam width decreases, the gain of the main lobe increases.

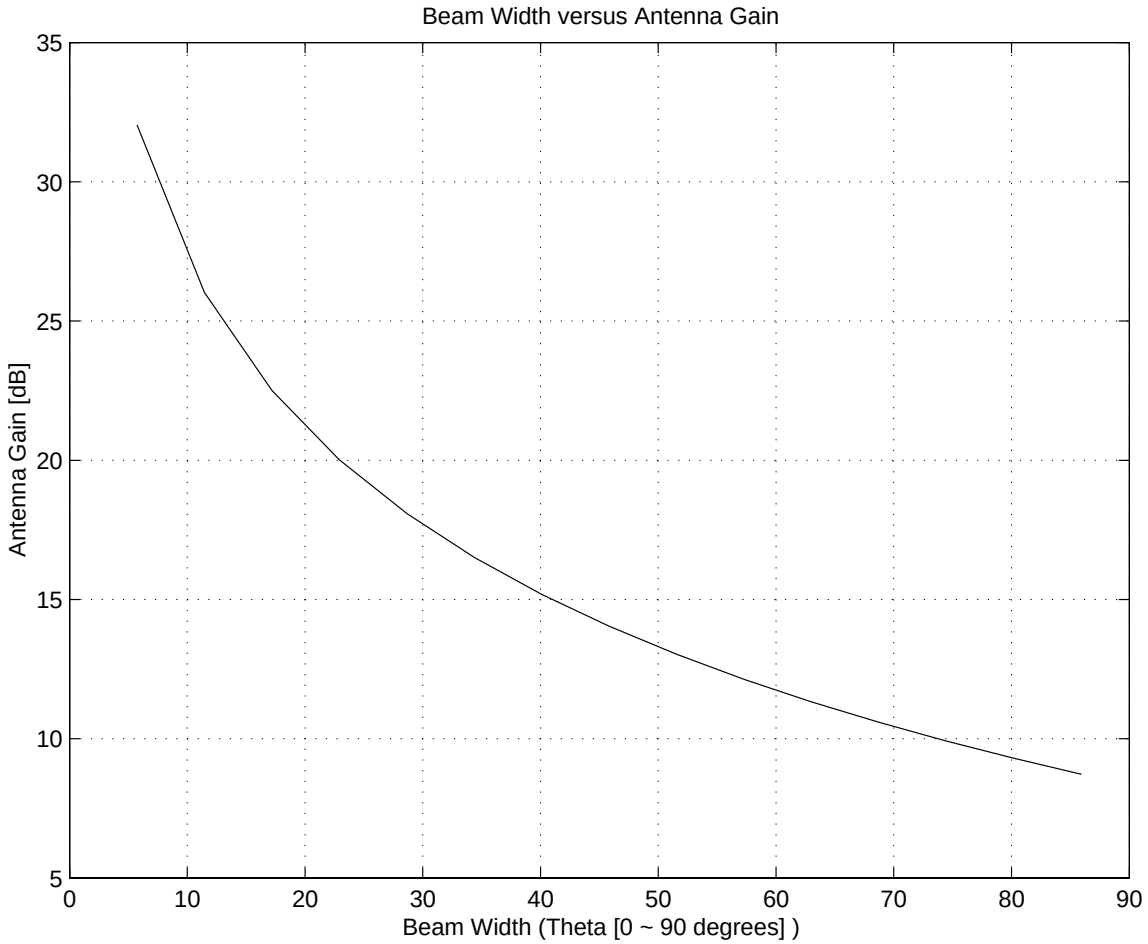

Figure 20: The impact of the beam width on the antenna gain.

Three locations are used to examine the effect of the user's beam width as shown in Figure 21. The results are explained as follows:

Near the base station: Increasing or decreasing θ does not have a noticeable impact on the throughput of the system. This is because the received SINR is large at this location. Therefore, regardless of having the interferers' signal in the main lobe or in the side lobes of the user's antenna, the cumulative received thermal noise plus the

interference power, with the exception of the dominant interferer, is too small to affect the received SINR. The dominant interferer, however, will always be received in the main lobe of the user's antenna regardless of the value of θ. Using adaptive modulation will always increase the throughput regardless of the user's beam width.

Near the middle of the sector: The throughput of the system decreases monotonically as θ increases. The degree of reduction varies for fixed modulations and adaptive modulation. This behavior is due to two factors: The first is the reduced signal power at the user of interest due to decreasing the antenna gain, as shown in Figure 20. The second is due to the fact that increasing θ will allow more interferers' power to be amplified by the main lobe gain of the user's antenna, which will result in reduced SINR at the user of interest. Adaptive modulation improves the throughput of the system compared with any single modulation.

Near the edge of the sector: The throughput shows a decaying behavior at this location versus θ. This behavior is due to the reduction of the antenna gain as the beamwidth increases. Any amplification for the interferences by the user's main lobe gain, as a result of increasing θ, will have a significant impact on the performance, i.e. will decrease the received SINR. This is, in part, due to reducing the received signal of interest by the path loss. Adaptive modulation will yield a better performance when the user's main lobe is between 2^o and 30^o. As the beam width increases above 30^o, the throughput for adaptive modulation will asymptotically approach that of the most robust modulation scheme, which is QPSK.

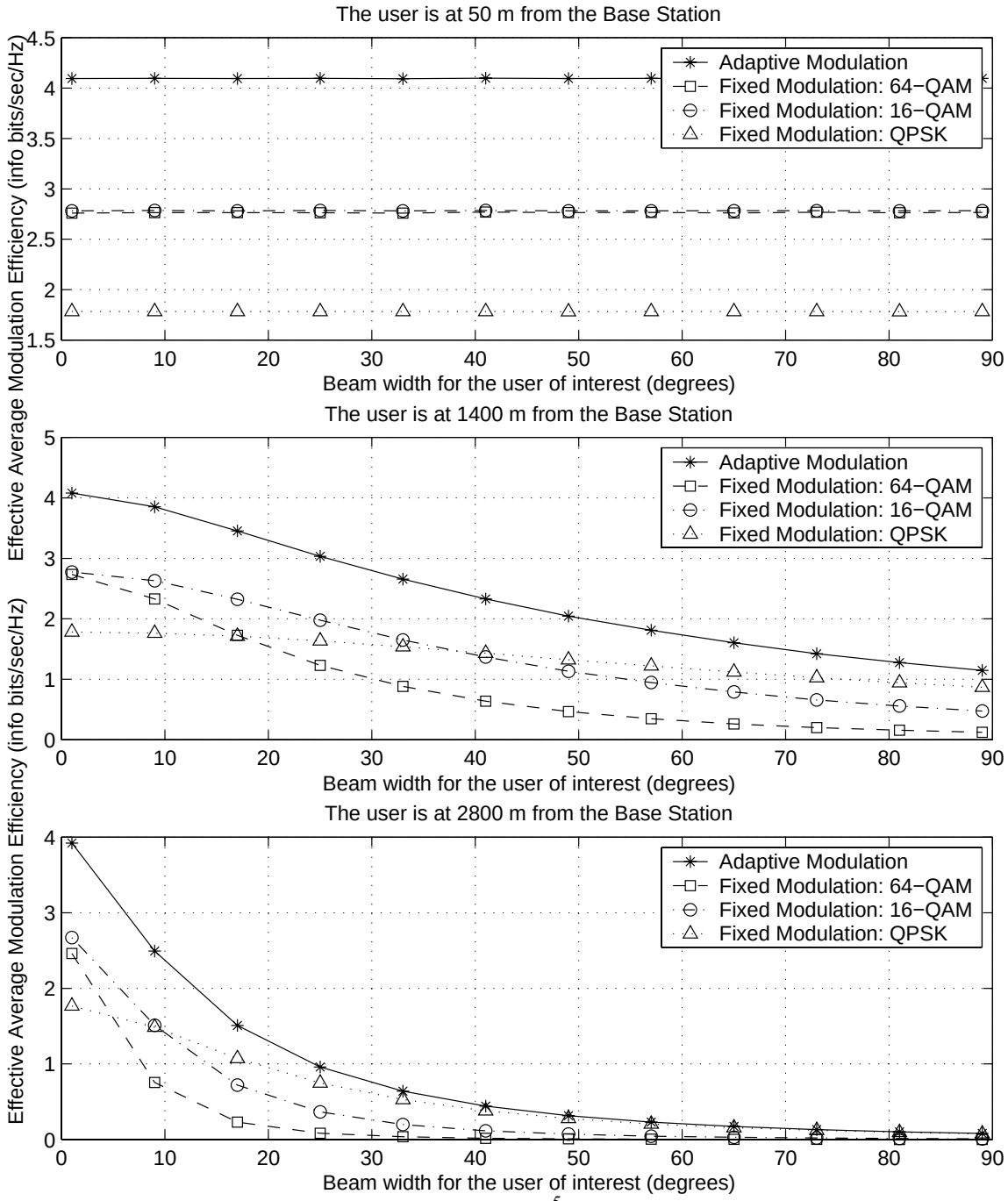

[Downlink transmission, f_c =2.5 GHz, BER =10^{-5}, T_x BW =6 MHz, T_x Power =200 mW, Rician parameter for the user of interest and the dominant interferer= 8, Rician parameter for the remaining interferers =3, Propagation exponent for the user and all the interferers =4, Std. Dev. of log normal shadowing =7 dB, Antenna beam width for the BS=90^o, Antenna gains for the B.S, the user of interest, and all the interferers: Main lobe =15 dB, Side lobes =-10 dB]

Figure 21: The impact of the user's antenna beam width on the system performance

4.5 Standard Deviation of Lognormal Shadowing

This section investigates the system response to standard deviation of lognormal shadowing, σ, and the results are shown in Figure 22. Adaptive modulation is used without error control coding or power control. The system response is investigated at three locations as follows:

Near the base station: As σ increases, the throughput for QPSK, 16-QAM, and adaptive modulation decreases, but the throughput for 64-QAM increases. This behavior is due to the fact that increasing σ will increase large-scale statistical variations, which will provide a higher chance of receiving a stronger signal from time to time. This phenomenon works in favor of 64-QAM, which requires larger SINR. Increasing the statistical variations will enhance the interference in case of using QPSK, 16-QAM, or adaptive modulation, which will result in decreasing the received SINR.

Near the middle of the sector: The throughput for 64-QAM and 16-QAM will improve with increasing σ; the throughput for QPSK will decrease. This behavior is similar to the behavior of the user near the base station. When adaptive modulation is used, the throughput increases as σ increases from 0 to 2 and then it levels off.

Near the edge of the sector: The throughput of the system improves as σ increases for all fixed modulations as well as adaptive modulation. This behavior is similar to the behavior near the base station.

Adaptive modulation improved the throughput everywhere in the sector, especially when σ increases.

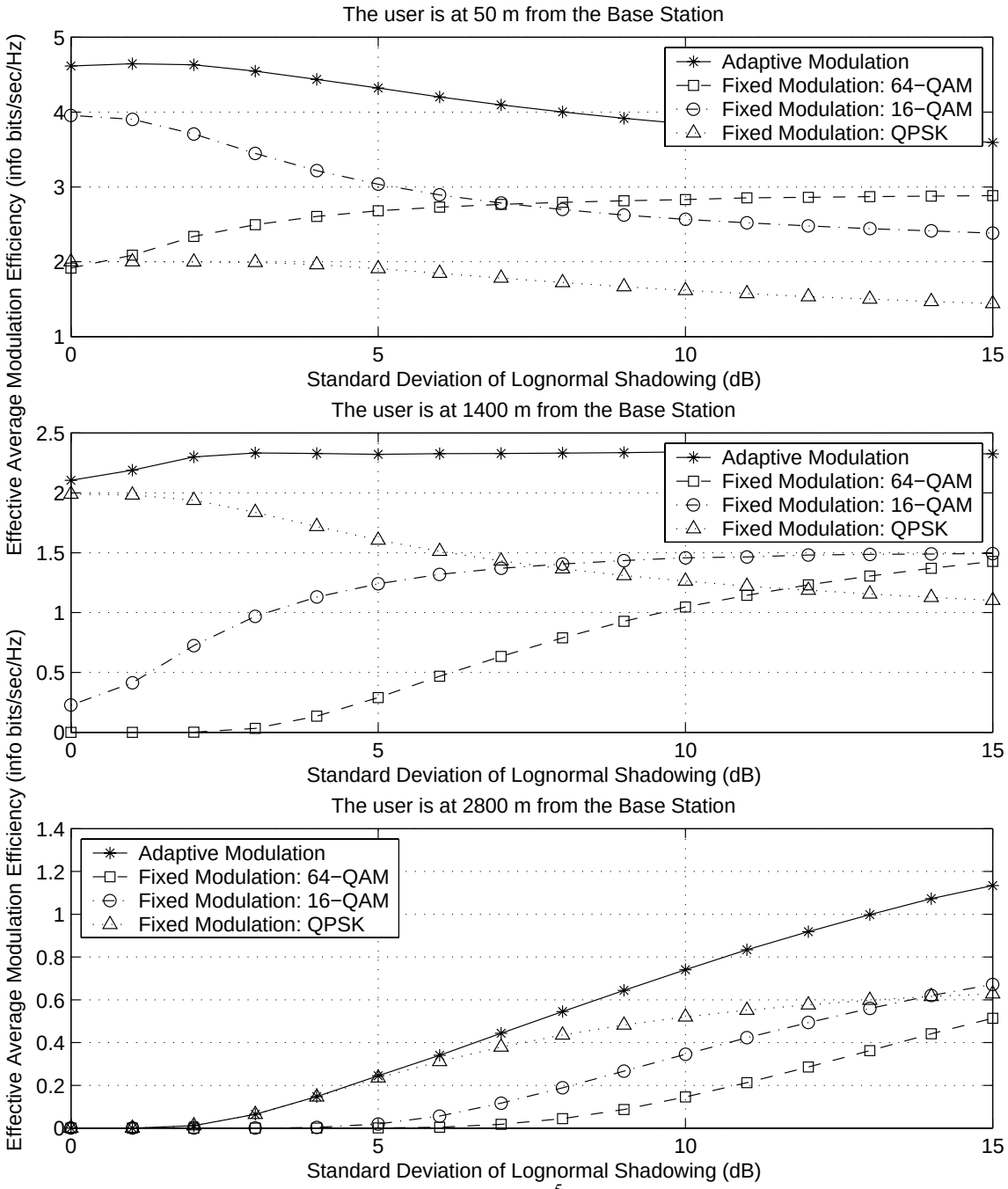

[Downlink transmission, f_c =2.5 GHz, BER =10^{-5}, T_x BW =6 MHz, T_x Power =200 mW, Rician parameter for the user of interest and the dominant interferer= 8, Rician parameter for the remaining interferes =3, Propagation exponent for the user and all the interferers =4, Antenna beam width for the BS=90^o, Antenna beam width for the user and all the interferers =30^o, Antenna gains for the B.S, the user of interest, and all the interferers: Main lobe =15 dB, Side lobes =-10 dB]

Figure 22: The Effect of Standard Deviation of Lognormal Shadowing

4.6 Transmission Bandwidth

The effect of the transmission bandwidth, ω, is investigated in this section and the results are shown in Figure 23. Adaptive modulation is used without error control coding or power control. The transmission bandwidth is considered in the range of 1 to 16 MHz. The results are summarized as follows:

Near the base station: The transmission bandwidth doesn't play a role in the throughput of the system, because the received signal for the user of interest is strong at this location. The thermal noise, which is proportional to the transmission bandwidth, increases linearly with ω. The resulting SINR, after increasing the thermal noise to its maximum value, meets the requirement for any fixed modulation and for adaptive modulation. Adaptive modulation provides a consistent advantage over any fixed modulation at this location.

Near the middle of the sector: The received signal for the user of interest decreases at this location due to increasing the path loss. Increasing the thermal noise, due to increasing ω, will have a significant impact on the evaluated SINR and, therefore, on the throughput, as shown in the middle graph of Figure 23. Adaptive modulation will increase the throughput for any ω value with greater increase for smaller ω.

Near the edge of the sector: The received signal for the user of interest is in its weakest value, due to the largest path loss. The effect of increasing the thermal noise will be significant at this location as shown in the bottom graph of Figure 23. As the ω increases the throughput for adaptive modulation asymptotically approaches the throughput of QPSK.

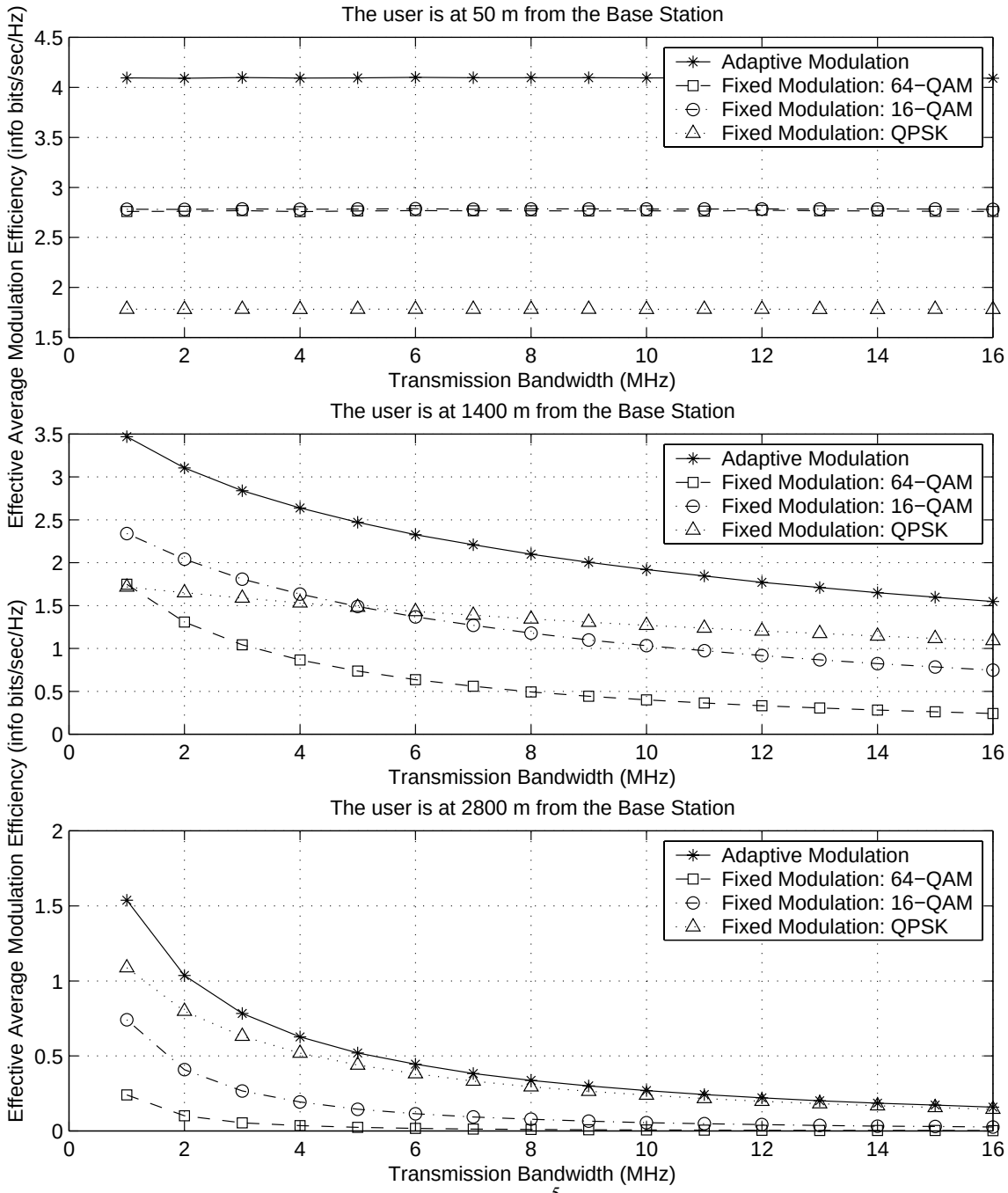

[Downlink transmission, f_c =2.5 GHz, BER =10^{-5}, T_x Power =200 mW, Rician parameter for the user of interest and the dominant interferer= 8, Rician parameter for the remaining interferes =3, Propagation exponent for the user and all the interferers =4, Std. Dev. of log normal shadowing =7 dB, Antenna beam width for the BS=90^o, Antenna beam width for the user and all the interferers =$30^{o,}$ Antenna gains for the B.S, the user of interest, and all the interferers: Main lobe =15 dB, Side lobes =-10 dB]

Figure 23: The Effect of the Transmission Bandwidth

4.7 Transmitted Power

The effect of the transmitted power, P_{tx}, on the throughput of the system is investigated in this section and the results are shown in Figure 24. Only adaptive modulation is used without error control coding or power control. The effect is examined by using three transmitted powers: 20 mW, 200 mW, and 2000 mW. The results are summarized as follows:

When P_{tx} = 20 mW: As the user is located further from the base station, the throughput will have an exponentially decaying-like performance. Near the base station, adaptive modulation performs better than any fixed modulation. Adaptive modulation will asymptotically approach the best performing fixed-modulation for users in the further half of the sector.

When P_{tx} = 200 mW: The throughput of the system is equivalent to the previous case for those users near the base station. If the user is located further from the base station, a noticeable advantage will be achieved compared to the previous case. That is because users far from the base station will receive higher SINR compared with the previous case.

When P_{tx} = 2000 mW: The throughput will increase for those users located far from the base station, especially near the edge of the sector. The reason here is the same as the previous case. QPSK achieves close to 2 bits/sec/Hz, its maximum possible throughput, for distances up to 1500 m. Users close to the base station do not benefit from increasing the transmitted power for them.

For any transmitted power, adaptive modulation will increase the throughput

compared with any fixed modulation.

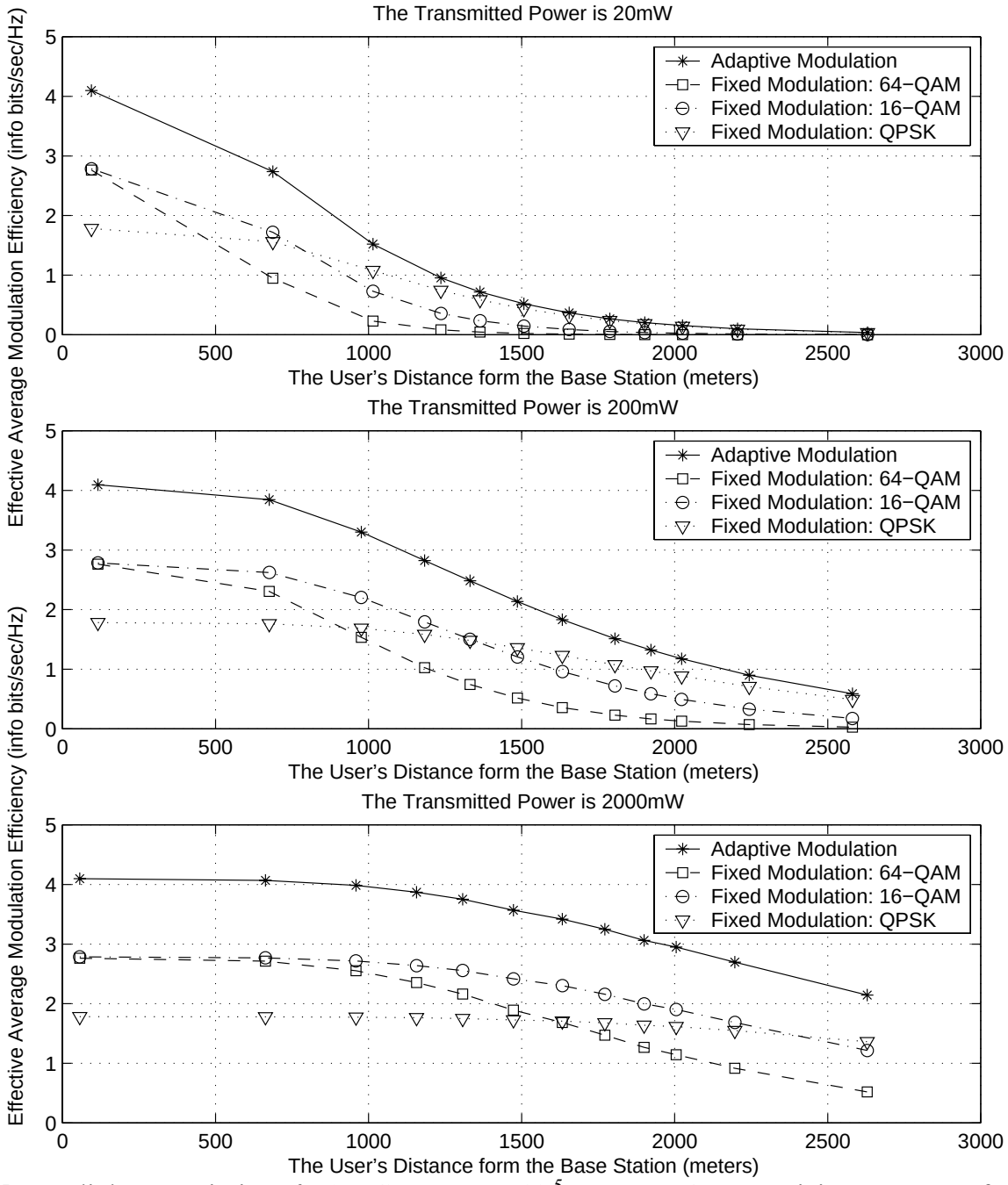

[Downlink transmission, f_c =2.5 GHz, BER =10^{-5}, T_x BW =6 MHz, Rician parameter for the user of interest and the dominant interferer= 8, Rician parameter for the remaining interferes =3, Propagation exponent for the user and all the interferers =4, Std. Dev. of log normal shadowing =7 dB, Antenna beam width for the BS=90^o, Antenna beam width for the user and all the interferers =30^o, Antenna gains for the B.S, the user of interest, and all the interferers: Main lobe =15 dB, Side lobes =-10 dB]

Figure 24: The effect of the Transmitted Power

Chapter 5: Simulation Results, Part 2

5.1 Introduction

In Chapter 4, the impacts of several parameters on the system performance were investigated. In all cases, adaptive modulation provided higher throughput than any fixed modulation. In this chapter, we investigate the advantages of combining adaptive-rate error control coding and/or power control with adaptive modulation. Figure 2 shows the flow chart for analyzing the performance of the system with several combinations of these techniques. This figure is summarized as follows:

We begin by investigating the system performance versus distance when adaptive modulation alone is used (Section 5.2). In Section 5.3, we compare the system performance when adaptive modulation alone is used versus the performance when a combination of adaptive modulation and error control coding (including adaptive coding) are used. In Section 5.4, the performance of the system that uses adaptive modulation is compared with another system that uses a combination of adaptive modulation and power control. The third comparison is shown in Section 5.5 is illustrated and achieved by comparing a system that uses adaptive modulation and adaptive coding versus another system that uses adaptive modulation and power control versus a third system that uses a combination of adaptive modulation, adaptive coding, and power control.

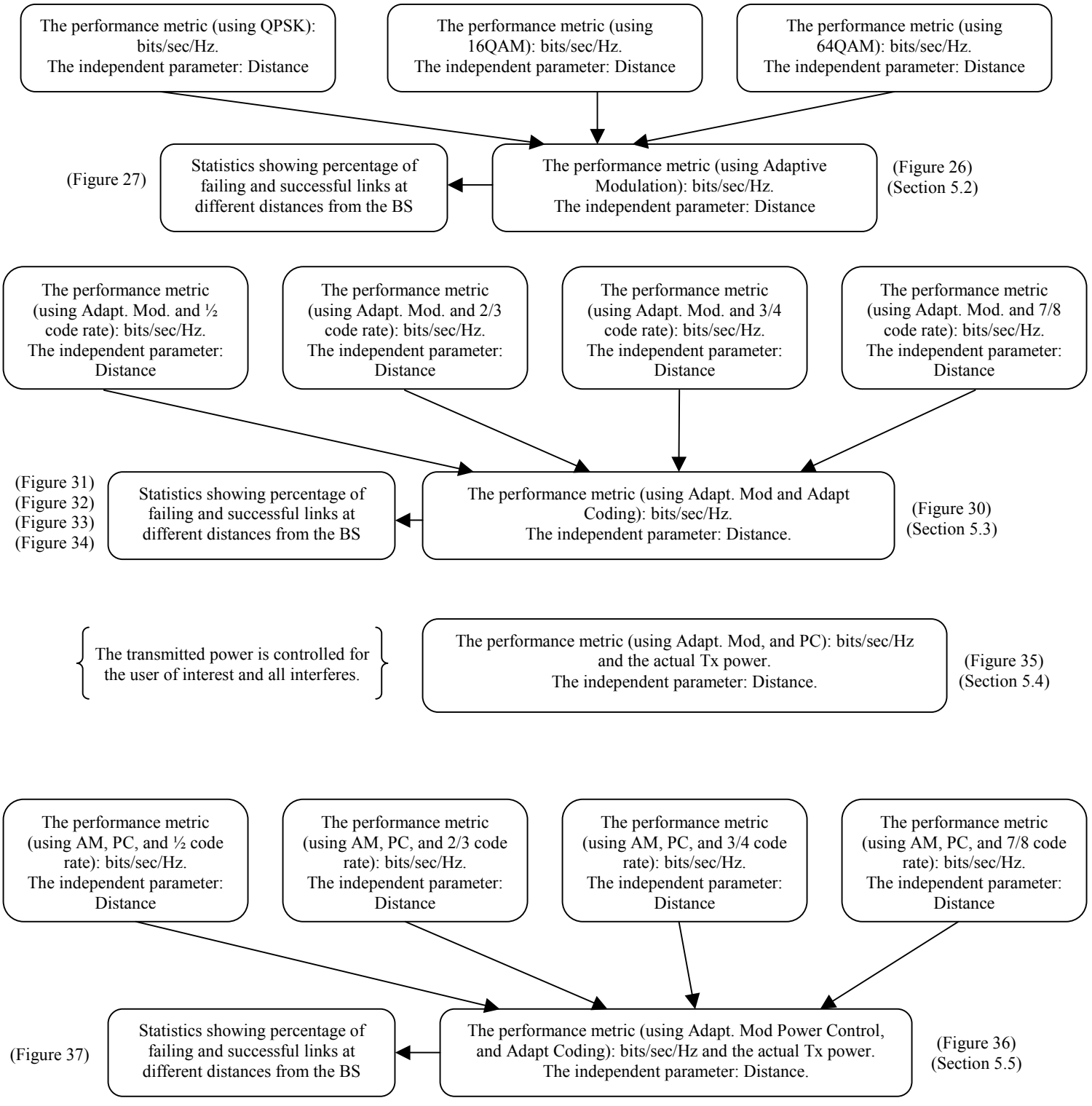

Figure 25: The impact of various parameters on the system performance (the throughput)

5.2 The effect of using adaptive modulation

The effect of using adaptive modulation throughout the sector as a function of the user of interest's distance from the base-station is investigated in this section, as shown in Figure 26. Adaptive modulation is used without error control coding or power control. All the interferers are placed in random positions. As the user of interest is located far from the base station, the system throughput will decrease as shown in the figure. Adaptive modulation improves the throughput everywhere in the sector. The best improvement is experienced near the base station, with 49% improvement in the throughput, compared with the best performing fixed modulation, 16-QAM. Near the edge of the sector, the performance improvement is about 5% compared with the best performing fixed modulation at this location, which is QPSK. This means that the adaptive modulator reverts to QPSK, most of the time, when far from the base station.

Figure 27 shows the percentage of time that each fixed modulation component is used, to form adaptive modulation, at several distances from the base station. The figure also shows the percentage of failing links throughout the sector. Several claims can be drawn from this figure. In each distance, the four data points add up to 100%. The received SINR is, at the best condition, near the base station. Therefore, the user transmits using 64-QAM, 46% of the time, 16-QAM, 23% of the time, and QPSK, 20% of the time. The link fails about 11% of the time. As the user of interest is located further from the base station, the received SINR will degrade due to several factors. The system will change the percentage of utilizing each fixed modulation in order to track the channel conditions. The degradation in the received SINR is reflected in increasing the percentage of failing links. Near the edge of the sector, QPSK is utilized most of the time,

17%, followed by 16-QAM, 3%, and 64-QAM, 1%. The percentage of failing links reaches the largest value near the edge of the sector, 79%. Figure 27 shows the reason for the superior performance of adaptive modulation compared with any fixed modulation. The adaptive modulation scheme selects one of several modulations to match the current conditions of the channel, and therefore, improving the overall throughput.

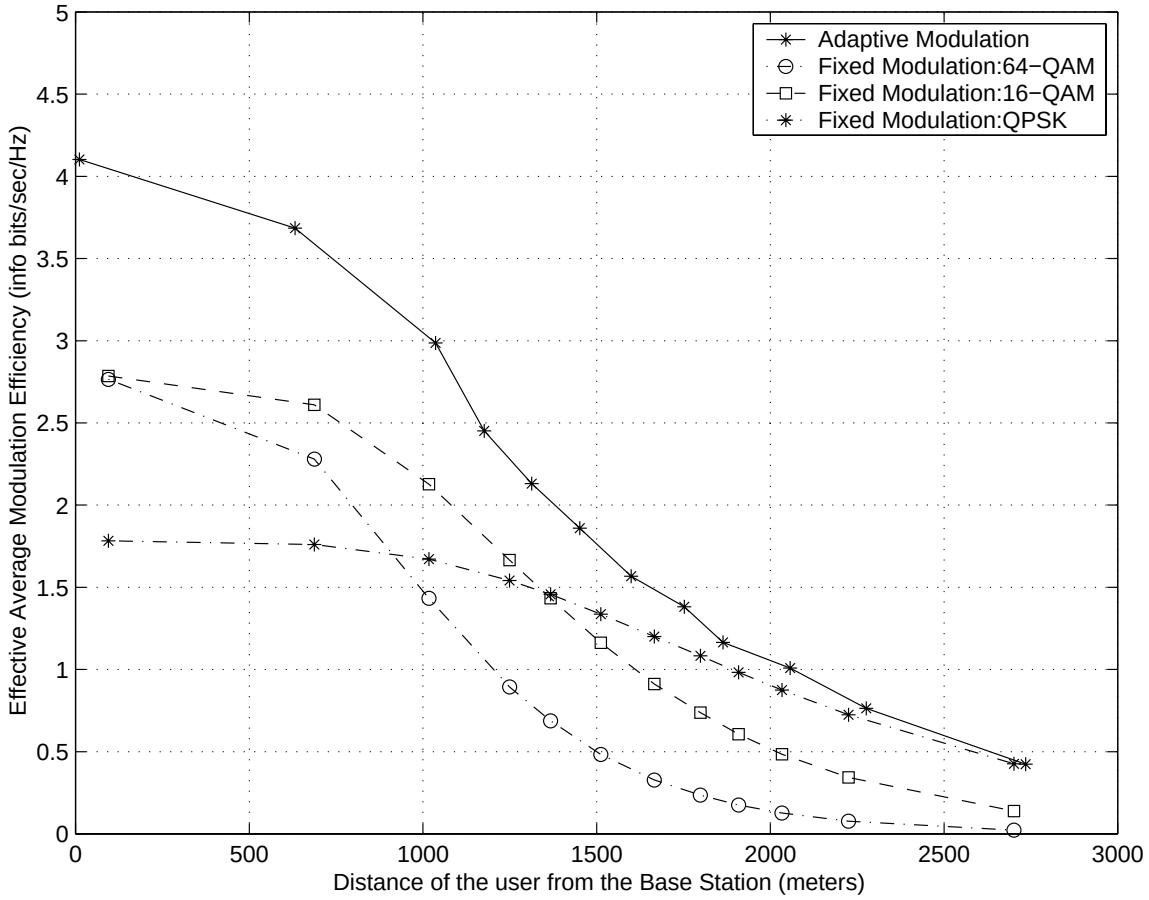

[Downlink transmission, f_c =2.5 GHz, BER =10^{-5}, T_x BW =6 MHz, T_x Power =200 mW, Rician parameter for the user of interest and the dominant interferer= 8, Rician parameter for the remaining interferers =3, Propagation exponent for the user and all the interferers =4, Std. Dev. of log normal shadowing =7 dB, Antenna beam width for the BS=90^o, Antenna beam width for the user and all the interferers =30^o, Antenna gains for the B.S, the user of interest, and all the interferers: Main lobe =15 dB, Side lobes =-10 dB]

Figure 26: The impact of using adaptive modulation on the system performance

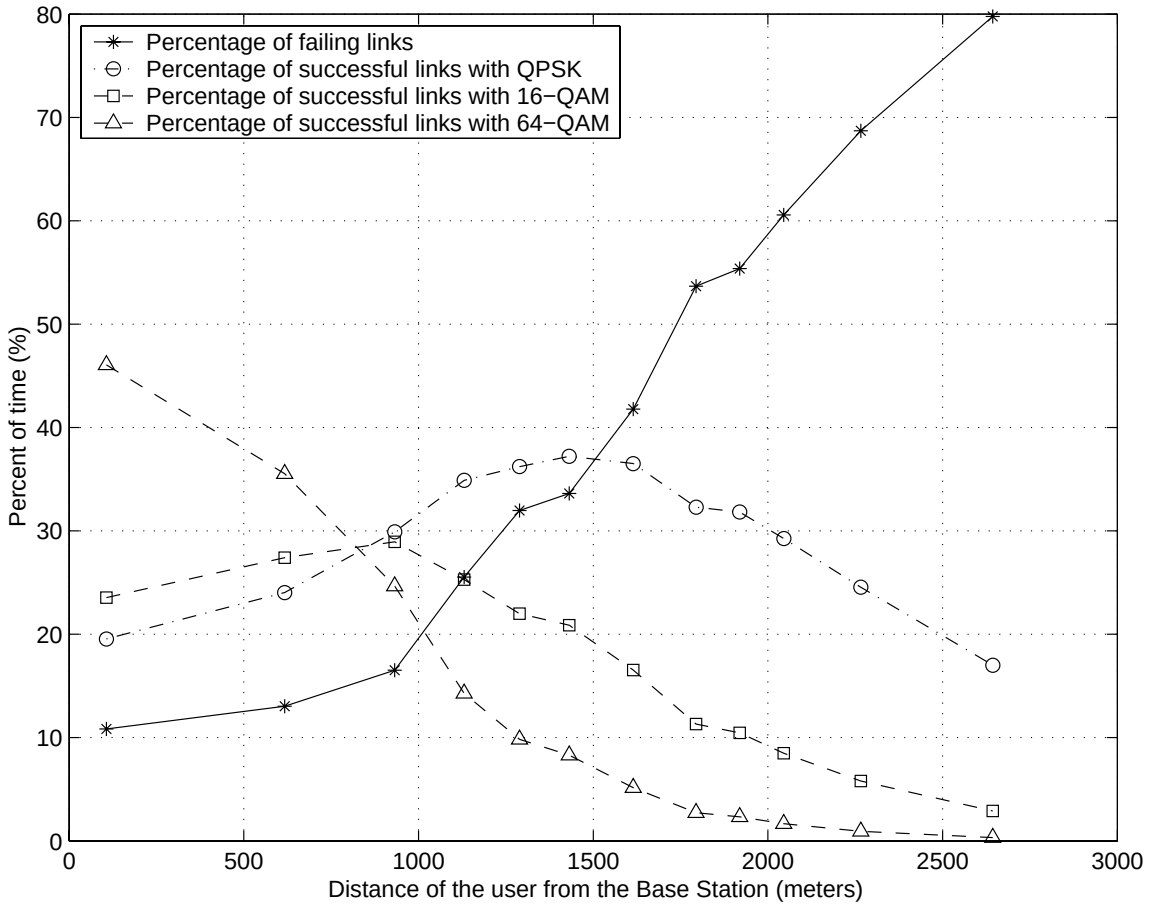

[Downlink transmission, f_c =2.5 GHz, BER =10^{-5}, T_x BW =6 MHz, T_x Power =200 mW, Rician parameter for the user of interest and the dominant interferer= 8, Rician parameter for the remaining interferers =3, Propagation exponent for the user and all the interferers =4, Std. Dev. of log normal shadowing =7 dB, Antenna beam width for the BS=90^o, Antenna beam width for the user and all the interferers =30^o, Antenna gains for the B.S, the user of interest, and all the interferers: Main lobe =15 dB, Side lobes =-10 dB]

Figure 27: Statistics of successful and failing links when adaptive modulation is used

Since the results presented here are statistical in nature, we will conduct a confidence check [39] in order to validate them.

Let $\hat{\theta}$ be the point estimate, of the parameter θ. For estimating θ, we obtain discrete-time output data of the form $\{Y_1, Y_2, ..., Y_n\}$ from the simulation. The point estimator or the sample mean of θ, $\hat{\theta}$, is then given by

$$\hat{\theta} = \frac{1}{n}\sum_{i=1}^{n} Y_i \qquad (1)$$

The point estimate $\hat{\theta}$ is said to be unbiased for θ if its expected value is θ. In other words, if

$$E(\hat{\theta}) = \theta \qquad (2)$$

But in general there is bias, b, in the point estimator, $\hat{\theta}$, where

$$E(\hat{\theta}) = \theta + b \qquad (3)$$

It is desirable to have estimators that are unbiased (b = 0), or as small bias b as possible relative to the magnitude of θ.

The length of the interval estimate is a measure of the error in the point estimate [39]. The interval estimate length requires calculating the variance of the point estimate $\hat{\theta}$. Let

$$\sigma^2(\hat{\theta}) = \text{var}(\hat{\theta}) \qquad (4)$$

represent the true variance of the point estimator $\hat{\theta}$, and let $\hat{\sigma}^2(\hat{\theta})$ represent an estimator of $\sigma^2(\hat{\theta})$ based on the data $\{Y_1, Y_2, ..., Y_n\}$. However, in general

$$E[\hat{\sigma}^2(\hat{\theta})] = B\sigma^2(\hat{\theta}) \qquad (5)$$

where B is the bias in the variance estimator. It is preferable to have B = 1, in

which case $\hat{\sigma}^2(\hat{\theta})$ is considered an unbiased estimate of the variance $\sigma^2(\hat{\theta})$. In this case the statistic

$$t = \frac{\hat{\theta} - \theta}{\hat{\sigma}(\hat{\theta})} \tag{6}$$

is *t*-distributed with *f* degrees of freedom. Providing that the following two conditions are met:

The point estimator $\hat{\theta}$ is an unbiased estimate of θ, ($b \approx 0$).

The estimator $\hat{\sigma}^2(\hat{\theta})$ is an unbiased estimator of $\sigma^2(\hat{\theta})$ ($B \approx 1$), providing that the output data $\{Y_1, Y_2, ..., Y_n\}$ are independent and identically distributed.

Therefore, an approximation for 100(1-α)% confidence interval for θ is given by

$$\hat{\theta} \pm t_{\alpha/2,f}\, \hat{\sigma}(\hat{\theta}) \tag{7}$$

or equivalently

$$\hat{\theta} - t_{\alpha/2,f}\, \hat{\sigma}(\hat{\theta}) \le \theta \le \hat{\theta} + t_{\alpha/2,f}\, \hat{\sigma}(\hat{\theta}) \tag{8}$$

where $t_{\alpha/2,f}$ is the 100(1-α) percentage point of a *t* distribution with *f* degrees of freedom. This value can be determined from table A.5 in [39]. The unbiased estimator of the variance is given as

$$\hat{\sigma}^2(\hat{\vartheta}) = \sum_{i=1}^{n} \frac{(Y_i - \hat{\theta})^2}{n(n-1)} \qquad (9)$$

The unbiased estimator of the mean, $\hat{\theta}$ and the unbiased estimator of the variance $\hat{\sigma}^2(\hat{\theta})$ are calculated at three positions in Figure 26: the first position (at 630 m from the BS), the second position (at 1450 m from the BS), and the third position (at 2276 m from the BS). These values are calculated using equations (1) and (9) over 100000 runs. The results are tabulated in Table 2.

Table 2: The mean and the variance for three user's positions from the BS

Distance from the BS (m)	630	1450	2276
Mean	3.81838	1.86612	0.77292
Variance	0.0174873	0.0156826	0.0107948

We calculate the-95% confidence interval for these positions as follows:

For first position (630 m from the BS): the 95-percentage point of a *t* distribution with ∞ (100000 – 1) degrees of freedom is 1.96 (table A.5 in [39]). Therefore, the confidence interval is calculated as

$3.81838 - 1.96\ (0.0174873) \leq \theta \leq 3.81838 + 1.96\ (0.0174873)$

In other words, with 95% confidence, the effective average modulation efficiency for a user located at 630 m from the BS should be in the interval

$3.78410 \leq \theta \leq 3.85266$

For the second position (1450 m from the BS): the 95-percentage point of a *t* distribution with ∞ (100000 – 1) degrees of freedom is 1.96 (table A.5 in [39]). Therefore, the confidence interval is calculated as

$$1.86612 - 1.96\,(0.0156826) \le \theta \le 1.86612 + 1.96\,(0.0156826)$$

In other words, with 95% confidence, the effective average modulation efficiency for a user located at 1450 m from the BS should be in the interval

$$1.83538 \le \theta \le 1.89686$$

For the third position (2276 m from the BS): the 95-percentage point of a t distribution with ∞ (100000 – 1) degrees of freedom is 1.96 (table A.5 in [39]). Therefore, the confidence interval is calculated as

$$0.77292 - 1.96\,(0.0107948) \le \theta \le 0.77292 + 1.96\,(0.0107948)$$

In other words, with 95% confidence, the effective average modulation efficiency for a user located at 2276 m from the BS should be in the interval

$$0.75176 \le \theta \le 0.79408$$

Since all the results are obtained from the same system model, with some modifications, we use the confidence check presented here as a measure of confidence for all the results.

5.3 The effect of combining adaptive modulation with coding

In this section, we investigate the effect of combining error control coding with adaptive modulation without using power control. In Section 5.2, we showed that adaptive modulation improves the throughput everywhere in the sector. Bit-Interleaved Coded Modulation (BICM) [38] is used for error control coding. An overview for BICM is given in Chapter 2. Adaptive modulation is combined with BICM of code rates 1/2, 2/3, 3/4, and 7/8. The system throughput is obtained for each combination everywhere in the sector. Adaptive modulation is also used with all code rates adaptively. In this case, the combinations of 4 code rates and 3 constellations form 12 cases to choose from. Figure 28 shows the approach for combining adaptive modulation and adaptive coding. The base station will use the appropriate combination of modulation and code rate to track the current channel condition. Combining coding with modulation will reduce the required SINR to achieve the same BER, but will reduce the received information bits as shown in Figure 29. This figure illustrates each combination of modulation and code, the number of received information bits for each combination, and the location of each combination on the SINR axis. The SINR axis corresponds to bit error rate of 10^{-5} in Figure 28. In some cases, a combination of modulation and code rate will yield more information bits, but requires less SINR than an adjacent combination. For example, the combination of 16-QAM and code rate 7/8 will yield 3.5 information bits/sec/Hz and requires less SINR than the combination of 64-QAM and code rate 1/2, which will yield 3.0 information bits/sec/Hz. This situation occurs three times as follows:

1. 16-QAM with code rate 2/3 (yields 2.67 information bits/sec/Hz) and QPSK with code rate 1 (yields 2.0 information bits/sec/Hz).

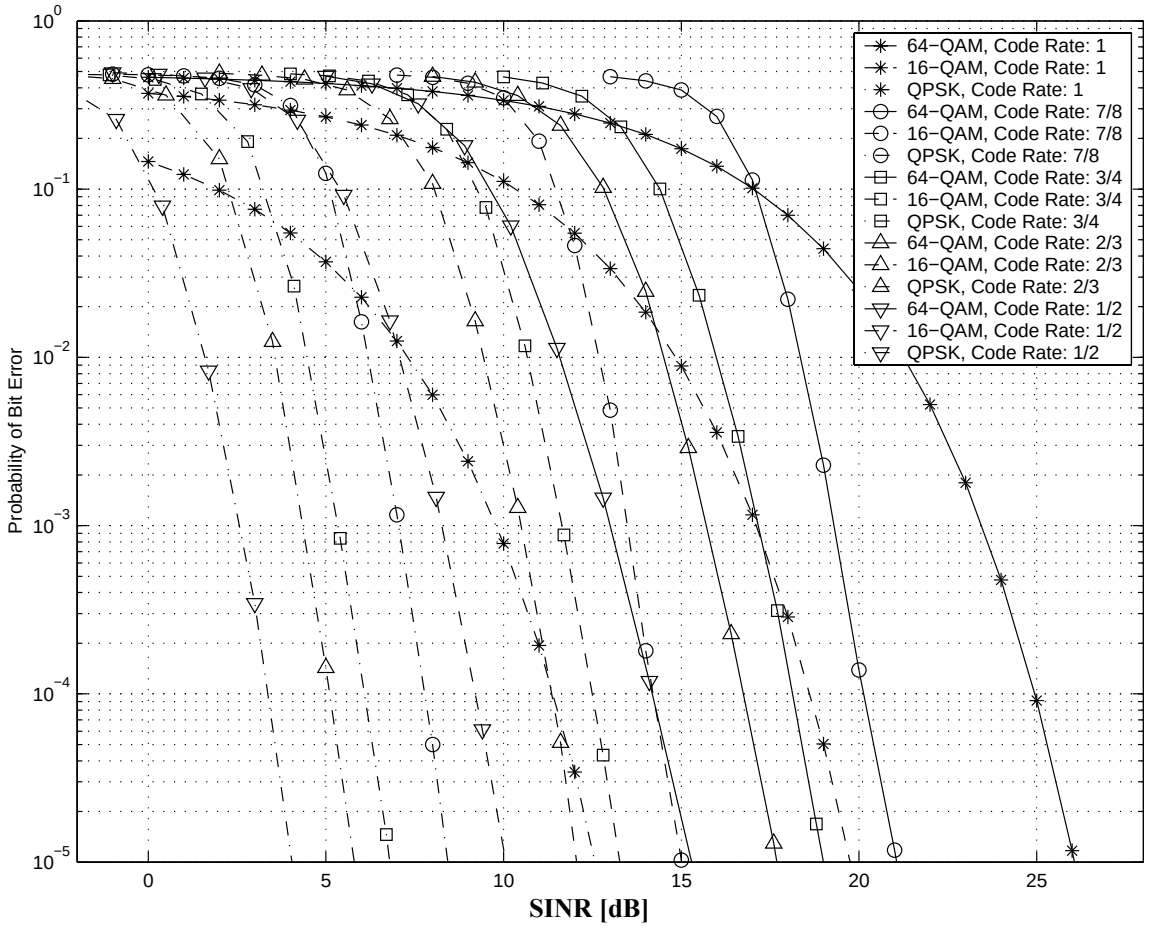

Figure 28: Probability of Bit Error for several combinations of code rates and modulations[2] (assuming the noise plus the interference have Gaussian distribution)

2. 16-QAM with code rate 7/8 (yields 3.5 information bits/sec/Hz) and 64-QAM with code rate 1/2 (yields 3.0 information bits/sec/Hz).

3. 64-QAM with code rate 3/4 (yields 4.5 information bits/sec/Hz) and 16-QAM with code rate 1 (yields 4.0 information bits/sec/Hz).

When this situation occurs, the base station will select the combination of modulation and code that will yield higher information bits/sec/Hz (and requires less SINR). According to this approach, three combinations will not be used at all and the

[2] These combinations determine the thresholds for adaptive modulation and adaptive coding. Reference: The data used to generate this figure were provided by Dr. Sirikiat Lek Ariyavisitakul, Radia Communications, Norcross, GA, USA

system will select from 12 different combinations.

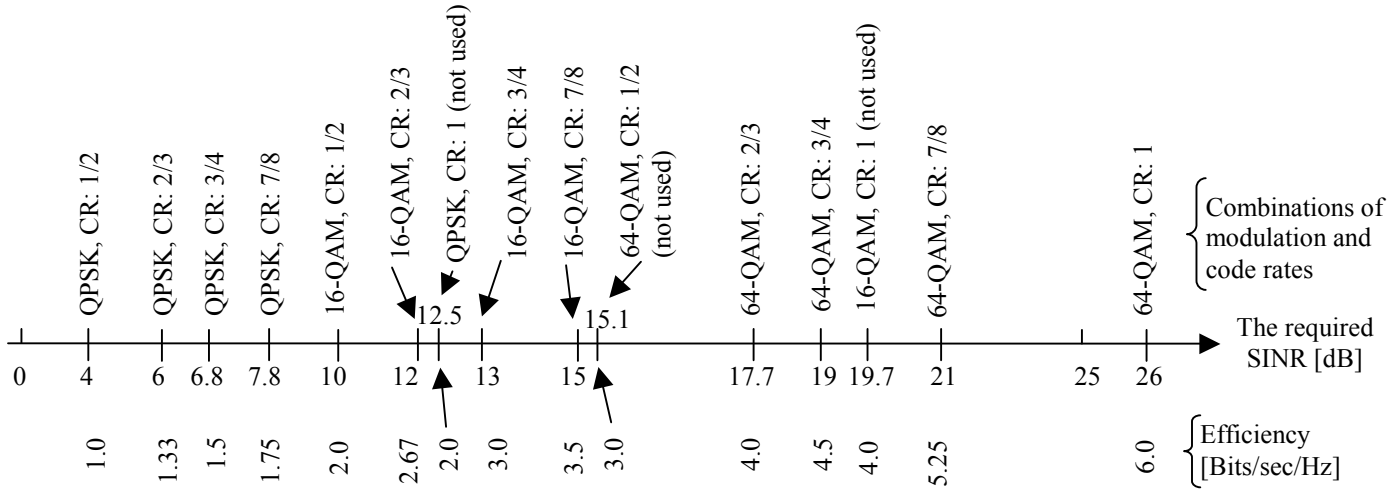

Figure 29: Combinations of modulation and code rates and the corresponding number of received information bits that will yield BER of 10^{-5}

Figure 30 shows the effect of combining BICM with adaptive modulation throughout the sector as a function of the user of interest's distance from the base-station. All the interferers are placed in random positions. When BICM with code rate 1/2 is combined with adaptive modulation, the system throughput will improve in the further half of the base station. The system throughput will degrade as the user equipment is located closer to the base station. Near the base station, the combination of code rate 1/2 and adaptive modulation will yield a throughput that is 34% less than adaptive modulation alone. The reason for this degradation is because code rate 1/2 will reduce the received information bit by a factor of 1/2. The signal quality at this location is strong enough to be detected without losing 1/2 of the received bits for coding. A similar trend applies for BICM [38] with code rates 2/3 and 3/4. However the amount of loss near the base station decreases for code rates 2/3 and 3/4 because of the reduction of redundant information required for them. When BICM with code rate 7/8 is combined with adaptive modulation, an improvement will be observed everywhere in the sector, with better

improvement in the further half of the sector. The reason for this enhancement is because combining code rate 7/8 with adaptive modulation will reduce the required SINR to achieve BER of 10^{-5}. The required redundant bits to implement this code (1/8) will not offset the advantage that is introduced by reducing the required SINR.

Combining adaptive coding with adaptive modulation will give the best possible result because of the increase in the number of choices that are available to select from as the channel conditions change. The slight degradation in the performance of the combination of adaptive modulation and adaptive coding compared with adaptive modulation and ode rate 7/8 near the middle of the sector is due to statistical variations in the results of our simulation.

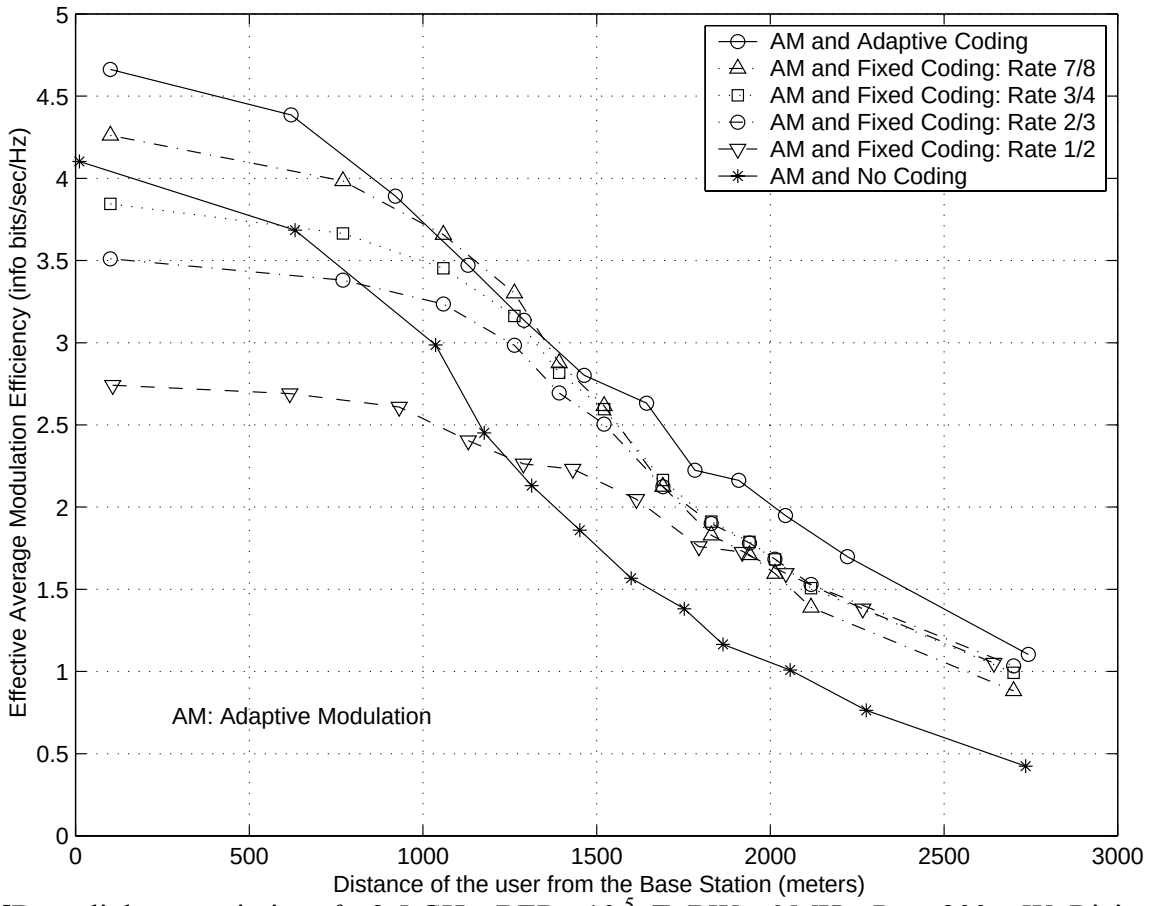

[Downlink transmission, f_c =2.5 GHz, BER =10^{-5}, T_x BW =6 MHz, P_{Tx} =200 mW, Rician parameter for the user of interest and the dominant interferer= 8, Rician parameter for the remaining interferers =3, Propagation exponent for the user and all the interferers =4, Std. Dev. of log normal shadowing =7 dB, Antenna beam width for the BS=90^o, Antenna beam width for the user and all the interferers =30^o, Antenna gains for the B.S, the user of interest, and all the interferers: Main lobe =15 dB, Side lobes =-10 dB]

Figure 30: The impact of using combined adaptive modulation and adaptive coding on the system performance

Figure 31 provides insight on the performance of combined adaptive modulation and adaptive coding. The figure shows the percentage of time in which a combination of a code rate and a modulation are selected in all areas of the sector. Furthermore, the figure illustrates the percentage of time in which the link failed to meet the requirement of the least SINR threshold everywhere in the sector.

Near the base station, the received SINR is high enough to select 64-QAM without coding 46% of the time. The combination of 64-QAM with code rate 7/8 is selected 18% of the time. The remaining combinations of modulation and code rate were selected 34.03% of the time and the link failed only 1.97% of the time. As the user equipment is located further from the base station, the received SINR will degrade, mainly due to increasing the path loss. The percentages of time for using different combinations at several locations in the sector are shown in Figure 31. As the user equipment is located further from the base station, the combinations that require high SINR, such as 64-QAM without coding, will be used less often while those which require less SINR, such as QPSK with code rate 1/2, will be used more often. The percentage of the failing links will increase near the edge of the sector to 39.02%.

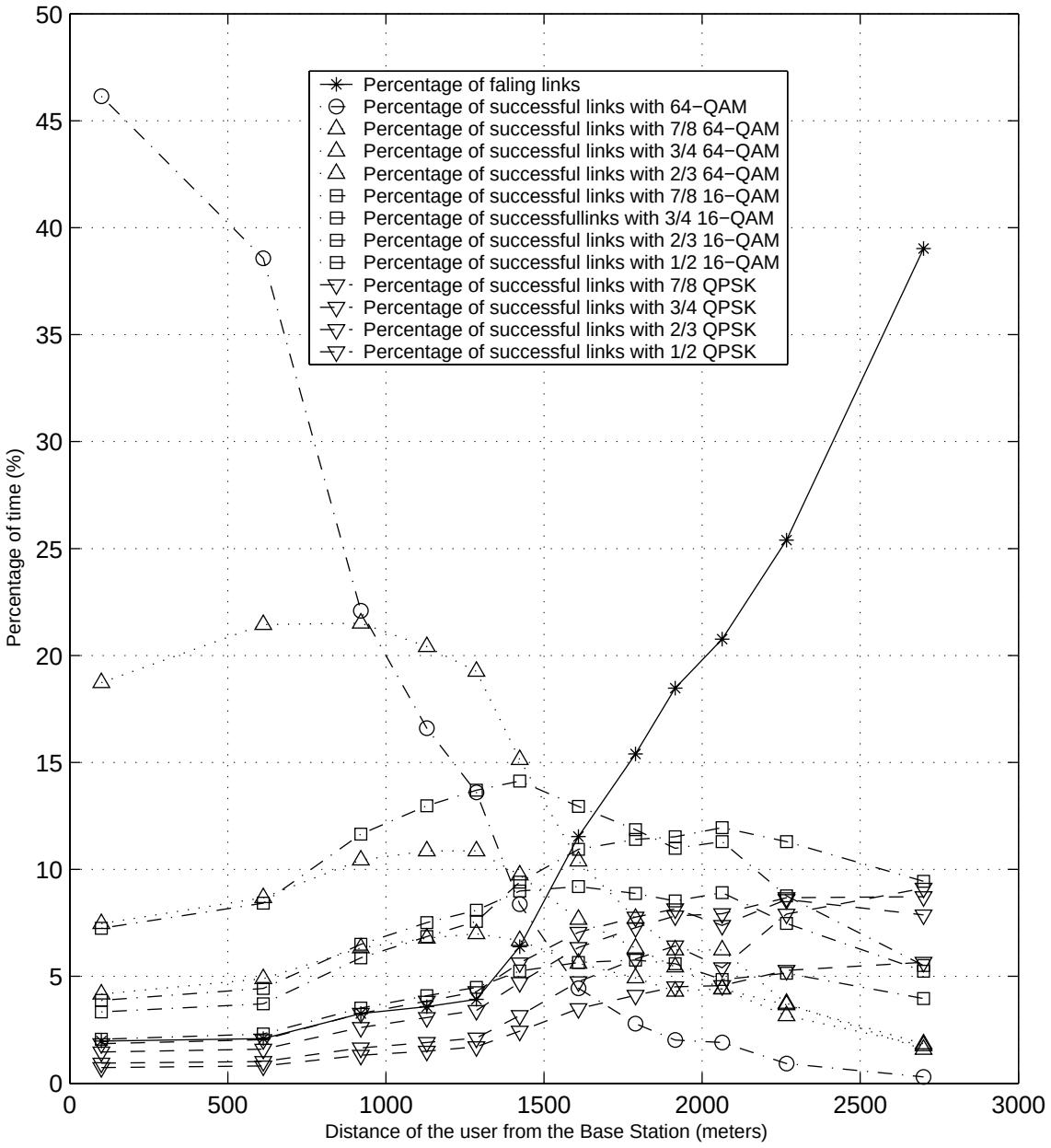

[Downlink transmission, f_c =2.5 GHz, BER =10^{-5}, T_x BW =6 MHz, T_x Power =200 mW, Rician parameter for the user of interest and the dominant interferer= 8, Rician parameter for the remaining interferers =3, Propagation exponent for the user and all the interferers =4, Std. Dev. of log normal shadowing =7 dB, Antenna beam width for the BS=90^o, Antenna beam width for the user and all the interferers =30^o, Antenna gains for the B.S, the user of interest, and all the interferers: Main lobe =15 dB, Side lobes =-10 dB]

Figure 31: Statistics of successful and failing links when adaptive modulation is combined with adaptive coding

Figure 32, 33, and 34 show the percentage of time for using a combination of code and modulation at three locations from the base station: 100 m, 1400 m, and 2700m.

At 100 meters from the base station: Combinations of 64-QAM and code rates 1, 2/3, 3/4, and 7/8, are used most of the time as shown in Figure 32. Combinations of 16-QAM and code rates 1/2, 2/3, 3/4, and 7/8 are used much less than the combinations of 64-QAM. Combinations of QPSK and code rates 1/2, 2/3, 3/4, and 7/8 are used very seldom compared with the combinations of 64-QAM and 16-QAM. The combination of 64-QAM with code rate 1/2 yields 3 information bits/sec/Hz and requires higher SINR than the combination of 16-QAM and code rate 7/8, which yield 3.5 information bits/sec/Hz, as shown in Figure 29. Therefore, the combination of 64-QAM and code rate 1/2 will not be used (the percentage of using this combination is zero in Figure 32). The same argument applies for QPSK with code rate 1 and 16-QAM with code rate 1. The successfully received links are 98.03 % of the transmitted links.

Near the middle of the sector: The combinations of modulation and coding are shown in Figure 33. The percentage of using combinations of constellation sizes and code rates will take different forms from the previous case to match the channel conditions at this location. The combination of 64-QAM with code rate 1 will be used less than the user near the base station. The combinations of 64-QAM, 2/3, 3/4 and 7/8 will also be used less often than those near the base station. The combinations of 16-QAM with code rates 1/2, 2/3, 3/4, and 7/8 will be used more often at this location than the previous location. The reason for this increase is because the best utilization for the channel will be through using combinations of 16-QAM and various code rates. Combinations of QPSK and code rates 1/2, 2/3, 3/4, and 7/8 will be used more than those near the base station. Three combinations are not used at all, similar to the previous case. These combinations

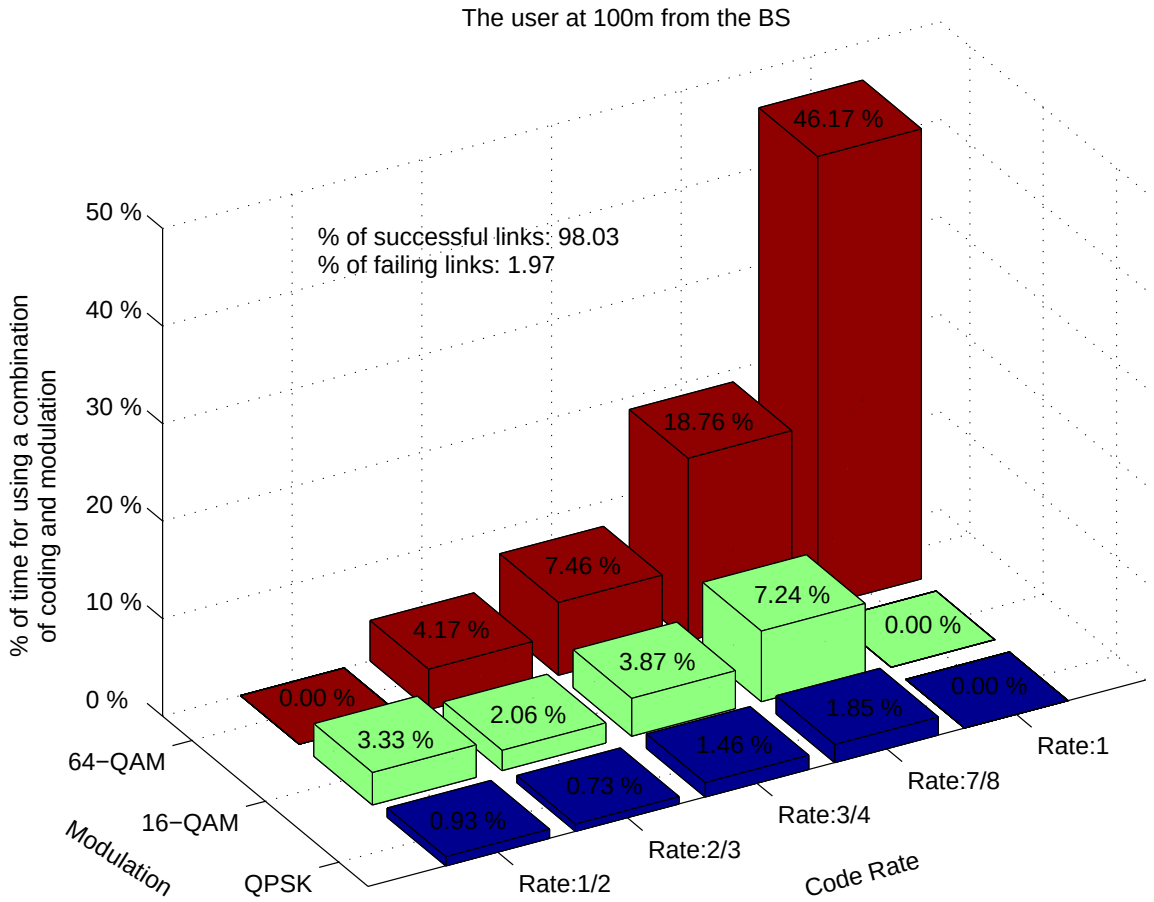

[Downlink transmission, f_c =2.5 GHz, BER =10^{-5}, T_x BW =6 MHz, T_x Power =200 mW, Rician parameter for the user of interest and the dominant interferer= 8, Rician parameter for the remaining interferers =3, Propagation exponent for the user and all the interferers =4, Std. Dev. of log normal shadowing =7 dB, Antenna beam width for the BS=90^o, Antenna beam width for the user and all the interferers =30^o, Antenna gains for the B.S, the user of interest, and all the interferers: Main lobe =15 dB, Side lobes =-10 dB]

Figure 32: Percentage of successful and failing links, 100 m from the base station

are 64-QAM with code rate ½, 16-QAM without coding and QPSK without coding. The successfully received links are 92.08 % of the transmitted links.

Near the edge of the sector: the user at this location will experience the worst channel condition due to path loss, shadowing, fading, and out-of-cell interference. Only 60.98% of the transmitted links are received successfully as shown in Figure 34.

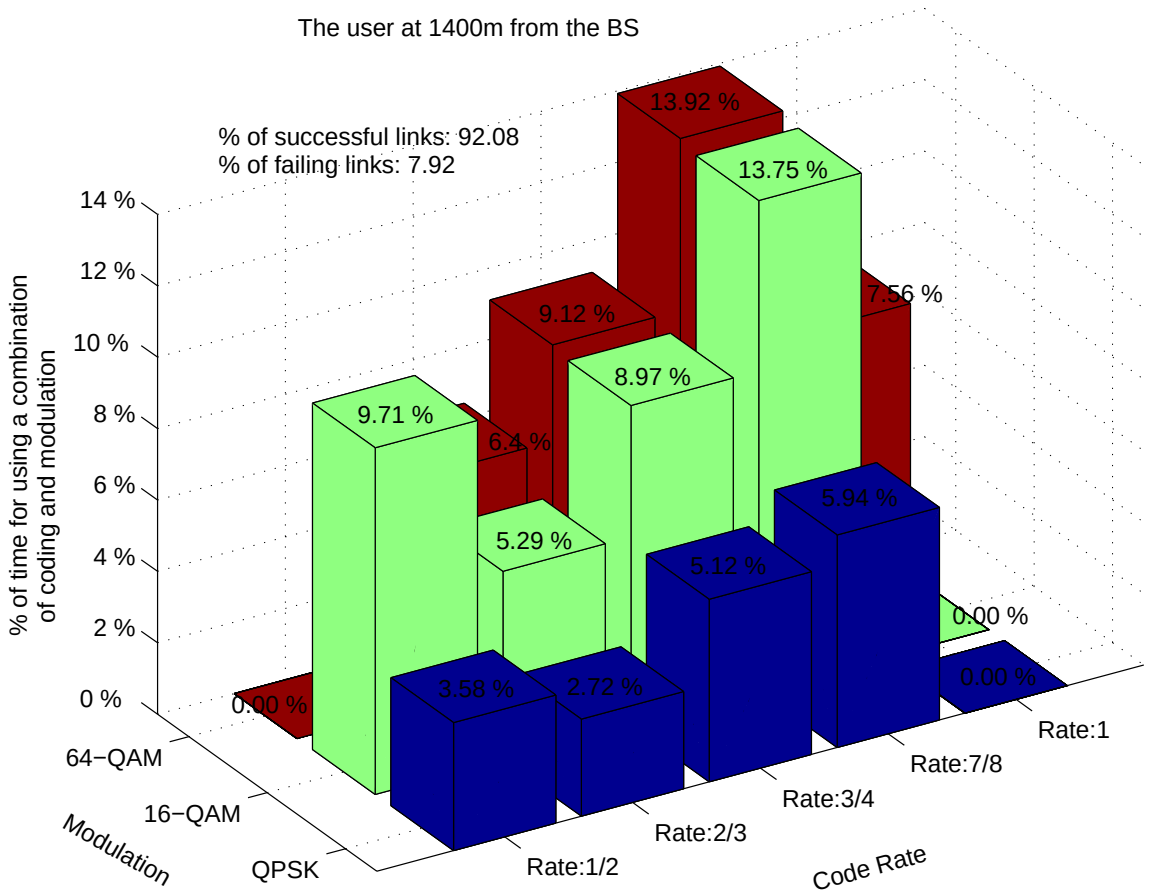

[Downlink transmission, f_c =2.5 GHz, BER =10^{-5}, T_x BW =6 MHz, T_x Power =200 mW, Rician parameter for the user of interest and the dominant interferer= 8, Rician parameter for the remaining interferers =3, Propagation exponent for the user and all the interferers =4, Std. Dev. of log normal shadowing =7 dB, Antenna beam width for the BS=90^o, Antenna beam width for the user and all the interferers =30^o, Antenna gains for the B.S, the user of interest, and all the interferers: Main lobe =15 dB, Side lobes =-10 dB]

Figure 33: Percentage of successful and failing links, 1400 m from the base station

The combinations of 64-QAM and code rates 1/2, 2/3, 3/4, and 7/8 will be used much less often than in the previous two cases. The combinations of 16-QAM with code rates1/2, 2/3, 3/4, and 7/8 will also be used less often than in the previous two cases. The combinations with QPSK and code rates 1, 2/3, 3/4, and 7/8 will be used more often than in the previous two cases. The combinations of QPSK will be used with approximately half of the successful links at this location. The remaining half is mostly used with

combinations of 16-QAM. Three combinations are not used at all, similar to the previous cases. These combinations are 64-QAM with code rate 1/2, 16-QAM without coding and QPSK without coding.

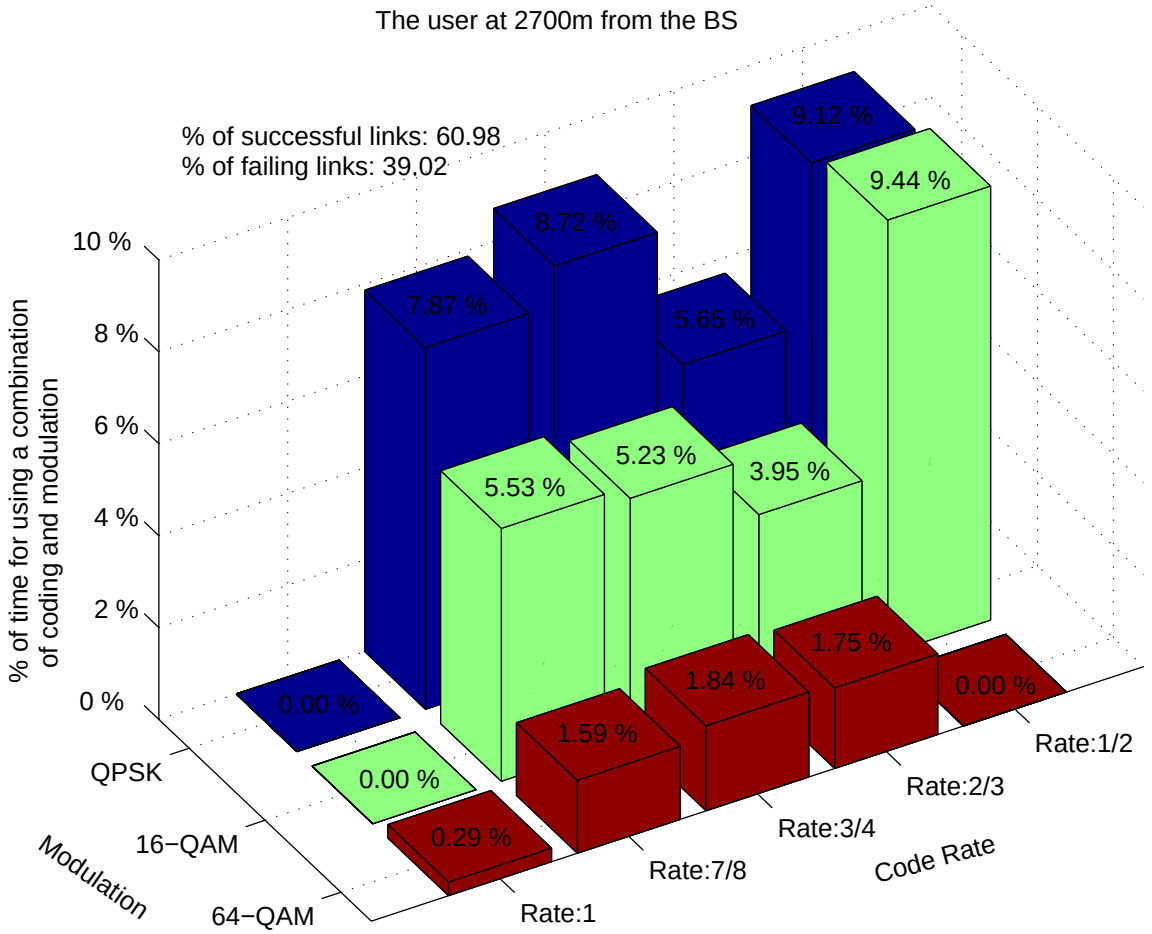

[Downlink transmission, f_c =2.5 GHz, BER =10^{-5}, T_x BW =6 MHz, T_x Power =200 mW, Rician parameter for the user of interest and the dominant interferer= 8, Rician parameter for the remaining interferers =3, Propagation exponent for the user and all the interferers =4, Std. Dev. of log normal shadowing =7 dB, Antenna beam width for the BS=90^o, Antenna beam width for the user and all the interferers =30^o, Antenna gains for the B.S, the user of interest, and all the interferers: Main lobe =15 dB, Side lobes =-10 dB]

Figure 34: Percentage of successful and failing links, 2700 m from the base station

5.4 The effect of combining power control with adaptive modulation

In this section, we examine the effect of combining power control with adaptive modulation, without using error control coding, throughout the sector as a function of the user of interest's distance from the base-station. All the interferers are placed in random positions. The results are shown in Figure 35. The performance of a combination of power control and adaptive modulation is compared with the performance of adaptive modulation alone in the top part of the figure. Combining power control with adaptive modulation will increase the throughput of the system throughout the sector. Users near the edge of the sector will experience a higher increase in the throughput, more than 0.5 bits/sec/Hz, than those near the base station, about 0.4 bits/sec/Hz.

The bottom part of Figure 35 shows the average transmitted power throughout the sector for both cases that are shown in the top part of the figure. When the system uses adaptive modulation alone, it will transmit a fixed power for all the users in the sector. If power control is combined with adaptive modulation, the transmitted power will be adjusted according to the needs of each user. The users near the base station will have a small path loss and therefore will require smaller transmitted power than those users near the edge of the sector. The bottom curve shows the average transmitted power throughout the sector when power control is combined with adaptive modulation.

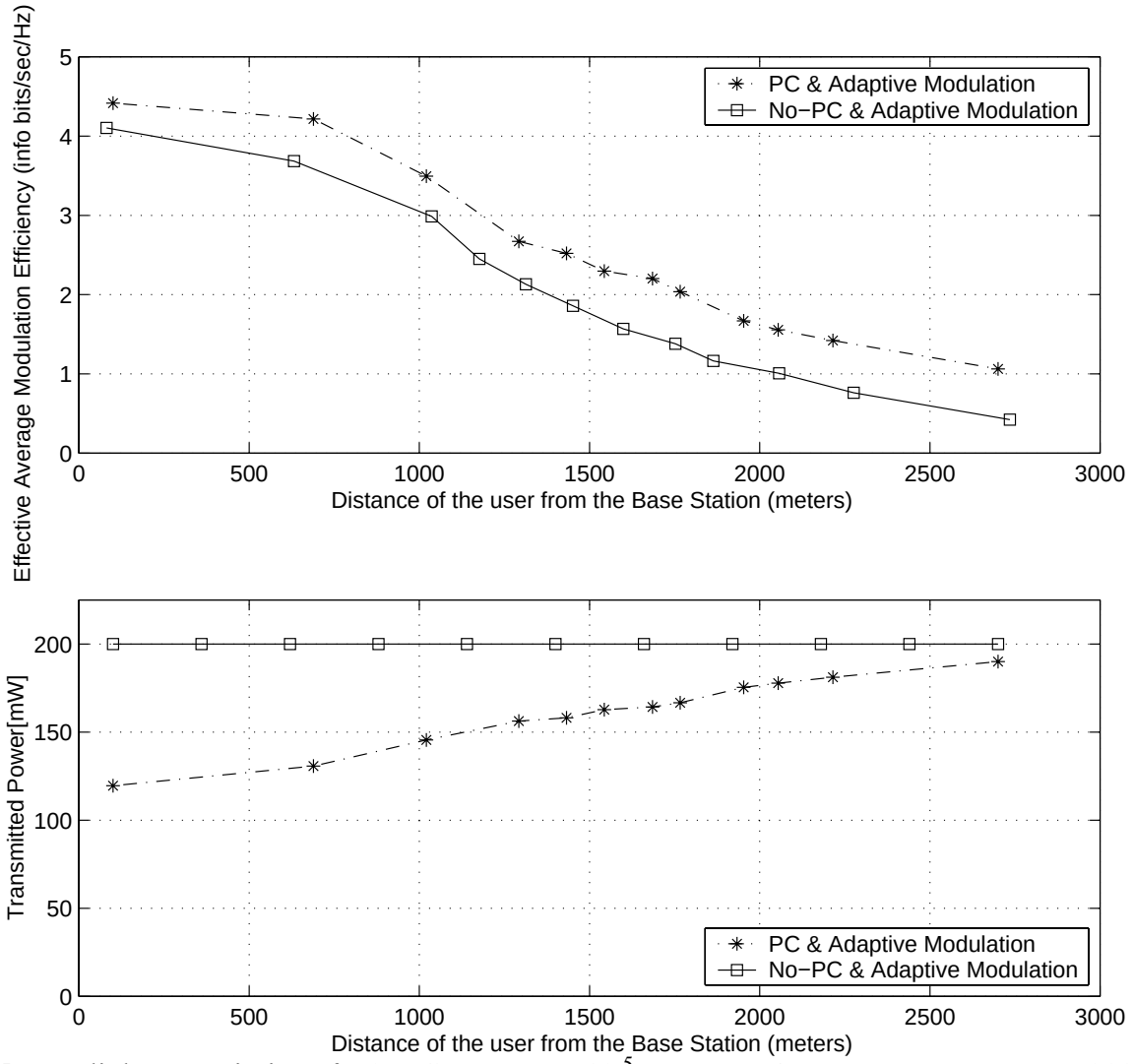

[Downlink transmission, f_c =2.5 GHz, BER =10^{-5}, T_x BW =6 MHz, Max.T_x Power =200 mW, Rician parameter for the user of interest and the dominant interferer= 8, Rician parameter for the remaining interferers =3, Propagation exponent for the user and all the interferers =4, Std. Dev. of log normal shadowing =7 dB, Antenna beam width for the BS=90^o, Antenna beam width for the user and all the interferers =30^o, Antenna gains for the B.S, the user of interest, and all the interferers: Main lobe =15 dB, Side lobes =-10 dB]

Figure 35: The impact of using combined adaptive modulation and power control on the system performance

5.5 The effect of combining adaptive coding and power control with adaptive modulation

The final case for evaluating the system performance examines the impact of combining power control and adaptive coding with adaptive modulation. The top part of Figure 36 shows the effective average modulation efficiency throughout the sector for all the cases that were considered so far: Fixed modulation using QPSK (without coding or power control), Adaptive modulation alone; combined adaptive modulation and adaptive coding; combined adaptive modulation and power control; and combined adaptive modulation, adaptive coding and power control. Several claims can be drawn from this figure. These claims are summarized as follows:

- A combination of adaptive modulation and adaptive coding will yield a throughput that is higher than adaptive modulation alone, everywhere in the sector.
- A combination of adaptive modulation and power control will yield a throughput that is higher than adaptive modulation alone, everywhere in the sector, but less than the previous case.
- The combination of adaptive modulation and adaptive coding will yield a higher throughput than the combination of adaptive modulation and power control everywhere in the sector.
- Combining power control with adaptive modulation and adaptive coding will yield little improvement on top of the improvement that was obtained by combining adaptive modulation with adaptive coding. This improvement may not justify the added complexity that will be introduced when power control is combined with adaptive modulation and adaptive coding.

The bottom part of the figure shows the corresponding average transmitted power for each case that was considered in the top part of the figure. Several claims can be drawn from this figure. These claims are as follows:

- When adaptive modulation is combined with adaptive coding, the base station will transmit the maximum amount of power for all the users in the sector. This scenario of operation will not take into account the advantage that is provided by the position of the user relative to the base station. The base station will transmit the maximum amount of power to the users that are near to it, even though they may not require all the transmitted power to receive a valid signal. This scheme will increase the interference to the user who is using the same frequency band in the adjacent sectors. Since all the users strive to achieve line of sight communication, if possible, and all base stations use sectored antennas, the dominant interferer will have the major impact on the system performance.

- When adaptive modulation is combined with power control, the base station will take advantage of the relative position of each user. An amount of power that is required for receiving a valid signal plus 10% safety margin will be transmitted from the base station. Therefore, users close to the base station will require about 40% less power in that case than the previous case. As the users are located further from the base station, the path loss will increase and the required transmitted power to achieve a valid signal will increase accordingly. Near the edge of the sector, the required transmitted signal is slightly smaller than the maximum power. Reducing the transmitted power will reduce the interference in the adjacent sectors, which is the main advantage for utilizing this scheme.

- When adaptive modulation is combined with adaptive coding and power control, the base station will have more combinations to choose from. The transmitted power will be adjusted to the appropriate combination plus 10%, similar to the previous case. This approach will yield an average transmitted power that is higher than in the previous case everywhere in the sector.
- Since the main objective in fixed wireless communication systems is to maximize the system throughput and since the transmitted power does not pose a major problem for fixed wireless communication system, the case of combined adaptive modulation and adaptive coding appears to be the most viable combination that provides the maximum throughput without the complexity that is added by combining power control.
- The case of using QPSK without coding or power control is included in Figure 36 to indicate the obtained gain (throughput) from the techniques that were mentioned above.

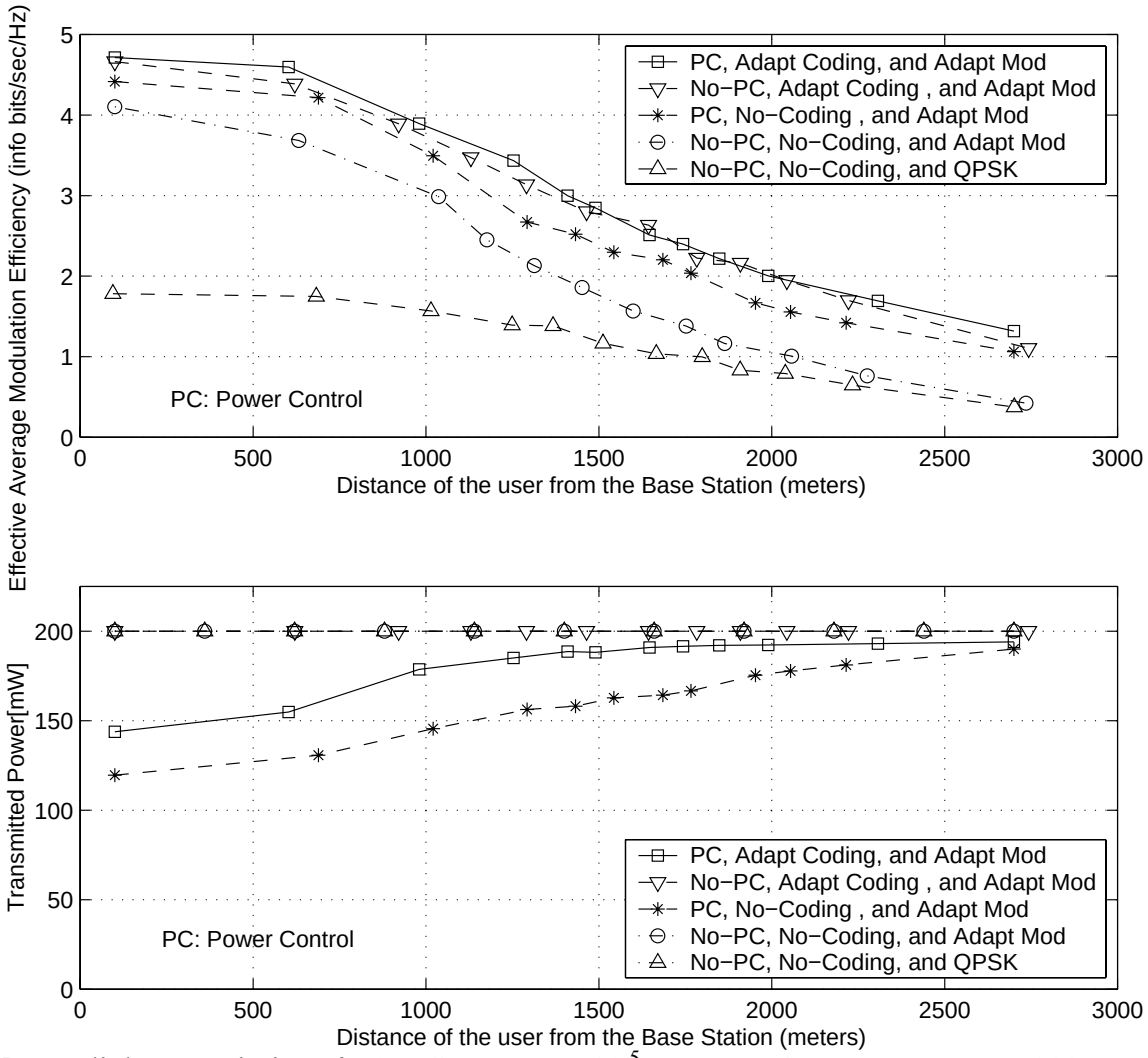

[Downlink transmission, f_c =2.5 GHz, BER =10^{-5}, T_x BW =6 MHz, T_x Power =200 mW, Rician parameter for the user of interest and the dominant interferer= 8, Rician parameter for the remaining interferers =3, Propagation exponent for the user and all the interferers =4, Std. Dev. of log normal shadowing =7 dB, Antenna beam width for the BS=90^o, Antenna beam width for the user and all the interferers =30^o, Antenna gains for the B.S, the user of interest, and all the interferers: Main lobe =15 dB, Side lobes =-10 dB]

Figure 36: The impact of using combined adaptive modulation, power control, and adaptive coding on the system performance

Figure 37 shows the percentage of using each combination of code and modulation throughout the sector. The figure also shows the percentage of the failing links everywhere in the sector. The base station utilizes 64-QAM with code rate 7/8 and 64-QAM with code rate 3/4, 47% and 19% of the time respectively, for nearby user equipments. The remaining usable combinations, including the failing links; will be used approximately 34% of the time at that location. As the user equipment is located far away from the base station, the combinations of code and modulation as well as the failing links will take the shape that is shown in Figure 37. Near the edge of the sector, the user equipment will use QPSK with code rate 1/2 about 24% of the time. This is the best combination at this location since the received SINR is at the smallest value. The link fails 24% of the time at this location. The remaining usable combinations are employed almost 52% of the time.

Comparing Figure 31 with Figure 37 provides an interesting insight for the impact of combining power control with adaptive modulation and power control. Figure 31 shows the statistics of successful and failing links when adaptive modulation and adaptive coding are coupled. Figure 37 shows the statistics of successful and failing links when adaptive modulation, adaptive coding, and power control are used together. Combining power control with adaptive modulation and adaptive coding will slightly reduce the percentage of failing links for user equipments near the base station. As the user equipment is located far from the base station, power control will reduce the percentage of failing links. The largest reduction in the percentage of failing links is observed near the edge of the sector. At this location, combining power control will reduce the failing links by 15%. This reduction, however, is not translated to larger

throughput. Combining power control with adaptive modulation and adaptive coding near the edge of the sector will increase the throughput by 0.2 information bits/sec/Hz. This increase is because the percentage of reduction in the failing links is used by the combination of QPSK and code rate 1/2, which yields 1 information bit/sec/Hz in each successful transmission. Averaging this improvement over all the transmissions will yield an improvement of 0.2 information bits/sec/Hz as indicated above.

This comparison also affirms our earlier conclusion that combining power control with adaptive modulation and adaptive coding does not improve the throughput significantly.

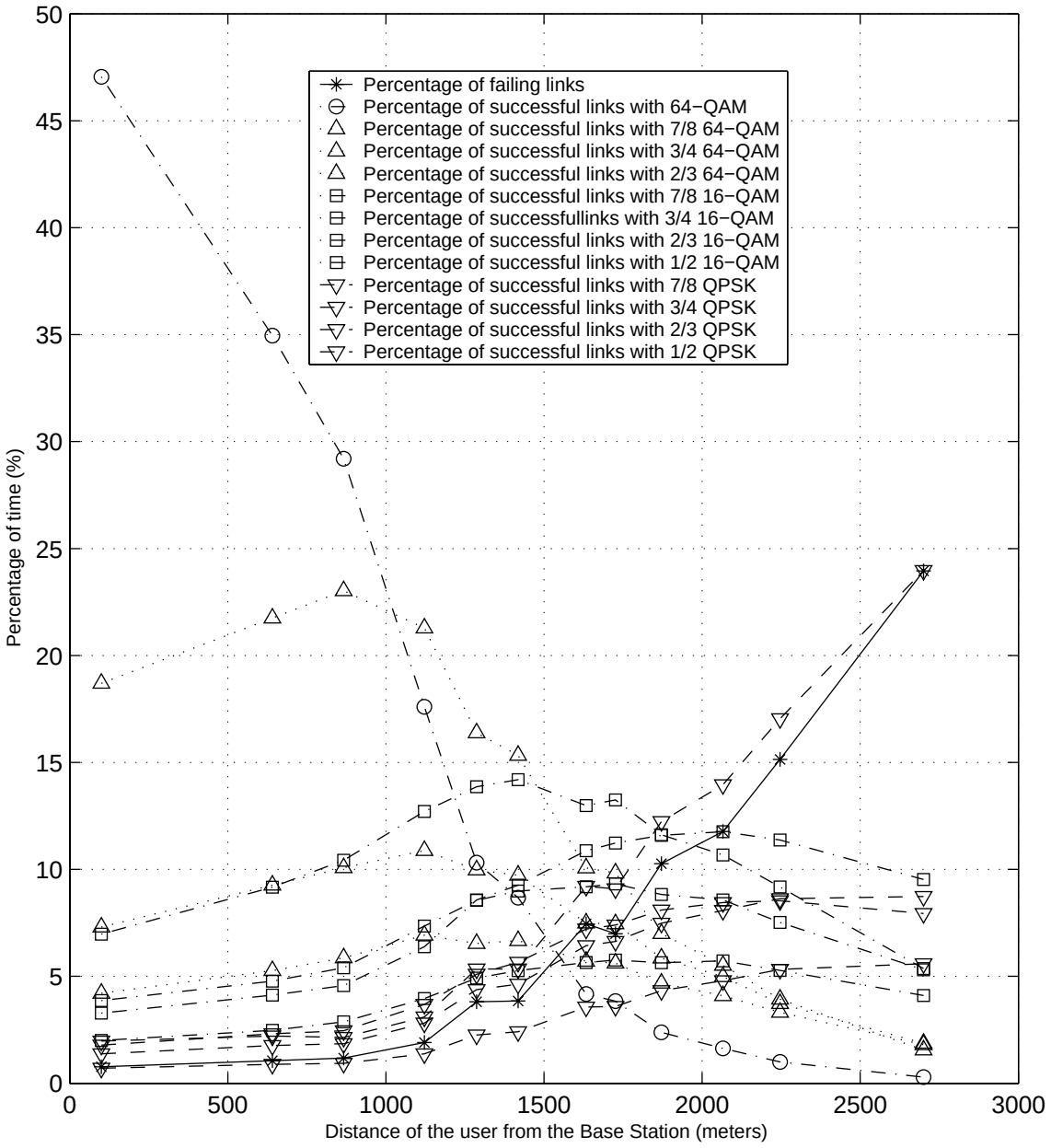

[Downlink transmission, f_c =2.5 GHz, BER =10^{-5}, T_x BW =6 MHz, T_x Power =200 mW, Rician parameter for the user of interest and the dominant interferer= 8, Rician parameter for the remaining interferers =3, Propagation exponent for the user and all the interferers =4, Std. Dev. of log normal shadowing =7 dB, Antenna beam width for the BS=90^o, Antenna beam width for the user and all the interferers =30^o, Antenna gains for the B.S, the user of interest, and all the interferers: Main lobe =15 dB, Side lobes =-10 dB]

Figure 37: Statistics for the successful and the failing links when combined adaptive modulation, power control, and adaptive coding are used

Chapter 6: Conclusions and Recommendations

6.1 Conclusions

Adaptive modulation, error control coding, and power control are well-known techniques in cellular mobile wireless communication systems. A comprehensive analysis for the advantage of applying these techniques in broadband cellular wireless communication systems is conducted in this research. Simulations are used for the evaluation in the downlink direction. A non line-of-sight system, represented by a propagation exponent of 4, is assumed to approximate a real system.

The evaluation began with a comparison of the throughput of three systems that utilize three different modulation schemes, QPSK, 16-QAM, and 64-QAM, with another system that utilizes adaptive modulation; i.e. a selection of QPSK, 16-QAM, or 64-QAM. Then two systems were compared: one that utilizes adaptive modulation and another that utilizes a combination of adaptive modulation and adaptive error control coding. Bit-Interleaved Coded Modulation is the error control-coding scheme used in this research. The third case compared a system that uses adaptive modulation and another that uses a combination of adaptive modulation and power control. The final case compared a system that uses a combination of adaptive modulation, adaptive error control coding, and power control with three systems: the first system uses adaptive modulation, the second system uses combination of adaptive modulation and adaptive error control coding, and the third system uses a combination of adaptive modulation and power control. The final case provided design guidelines for selecting the best combinations of adaptive techniques that will maximize the throughput in the downlink direction.

6.2 Summary of Contributions

In this work, several techniques were investigated to improve the performance, i.e. the throughput, in the downlink direction of fixed broadband cellular wireless systems. The results are summarized as follows:

1- Adaptive modulation was shown to provide performance gain throughout the sector, compared with any fixed modulation.

2- Combining adaptive coding, based on BICM, with adaptive modulation provides an extra gain on top of the gain that was obtained with adaptive modulation without coding, case (1). Users near the edge of the sector experience higher performance gain than those near the base station.

3- Combining power control with adaptive modulation provides performance gain similar to, but less than, the previous case.

4- Minimal performance gain, on top of the gain provided by case (2), is obtained when power control is combined with adaptive modulation and adaptive coding.

5- The gain provided in case (4) may not justify the complexity of using power control with adaptive modulation and adaptive coding. The latter two techniques provide an optimum performance in this setting.

6.3 Future Research

During the course of this research, the system model was as detailed and representative to an actual system as possible. However, in order to focus on analyzing our thesis problem, we simplified several issues that either do not have a direct impact on the downlink throughput of system or their impact is eliminated and left for consideration in the future research. In this section, we summarize various improvements that can be added to our system model, which will increase the complexity of the analysis and the accuracy of the results. We further suggest several techniques that can be considered to improve the throughput in the downlink direction.

The following factors can be added to our system model to have more accurate and representative results:

1- The cells, and sectors, of our system model are squared in shape. A hexagonal cellular system will be more representative of the actual system.

2- In the system model, we assumed that only one user equipment is randomly located in each sector. Therefore, adjacent channel interference is eliminated from our analysis. A more representative system model will include a random number of user equipments, with a limited maximum number, randomly located in each sector. This model will take into account the adjacent channel interference, which may have some impact on limiting the throughput on the downlink direction.

3- An ideal sectored antenna is assumed at the base station and the user equipment sides with an approximation on the received antenna gain at the user side as shown in chapter 3.

4- In our analysis, we assumed the channel response consists of one path. Incorporating a multipath channel model will provide more accurate representation of the system.

Some factors can be considered as a continuation of this research. Incorporating these factors may have an impact on improving the system performance. These factors, which are by no means complete, are as follows:

1- Investigating the effect of different coding schemes on the system performance, such as Convolutional coding or Turbo coding.

2- Investigating the effect of using an Interleaver, with several interleaving depths, together with the coding schemes mentioned in (1).

3- Investigating the effect of achieving line-of-sight between the base station and the customer premises' equipment by using relays or transponders, and the effect of this technique on the transmitted power, the resulting interference, and the throughput.

References

[1] S. Nanda, K. Balachandran, and S. Kumar, "Adaptation techniques in wireless packet data services," in *IEEE Commun. Mag*., vol. 38, no. 1, pp. 54-64, Jan. 2000.

[2] F. Babich, "Considerations on adaptive techniques for time-division multiplexing radio systems," *IEEE Trans. Veh. Tech*., vol. 48, no. 6, pp. 1862-1873, Nov. 1999.

[3] W. T. Webb and R. Steele, "Variable rate QAM for mobile radio," *IEEE Trans. Commun*., vol. 43, no. 7, pp. 2223-2230, July 1995.

[4] M. S. Alouini, X. Tang, and A. Goldsmith, "An Adaptive modulation scheme for simultaneous voice and data transmission over fading channels," in *Proc. IEEE VTC'98*, May 1998, pp. 939-943.

[5] K. Hamaguchi, Y. Kamio, and E. Moriyama, "Implementation and performance of an adaptive QAM modulation-level-controlled system for land mobile communications" in *Proc. IEEE VTC'97*, May 1997, pp. 1214-1218.

[6] Y. Kamio, S. Sampei, H. Sasaoka, and N. Norinaga, "Performance of modulation-level-controlled adaptive-modulation under limited transmission delay time for land mobile communications" in *Proc. IEEE VTC'95*, May 1995, pp. 221-225.

[7] X. Tang, M. S. Alouini, and A. Goldsmith, "Effect of channel estimation error on M-QAM BER performance in Rayleigh cading," in *Proc. IEEE VTC'99*, May 1999, pp. 1111-1115.

[8] A. Goldsmisth and S. G. Chua, "Adaptive coded modulation for fading channels," *IEEE Trans. Commun*., vol. 46, no. 5, pp. 595-602, May 1998.

[9] Y. M. Kim and W. C. Lindsey, "Adaptive coded-modulation in multipath fading channels" in *Proc. IEEE VTC'99*, May 1999, pp. 1795-1799.

[10] T. Ikeda, S. Sampei, N. Norinaga, "TDMA-based adaptive modulation with dynamic channel assignment for high-capacity communication systems," *IEEE Trans. On Vech. Commun*., vol. 49, no. 2, pp. 404-412, March 2000.

[11] S. Salamah, D. D. Falconer, and H. Yanikomeroglu, "Transmit Power Control in Fixed Cellular Broadband Wireless Systems,"in . *IEEE WCNC'00*, March 2000, pp. 624-628.

[12] B. Sklar, "Digital Communications – Fundamentals and Application," *P.T.R. Prentice Hall*, p.267, 1988.

[13] E. Zehavi, "8-PSK trellis codes for a Rayleigh channel," *IEEE Trans. Commun*., vol. 40, pp. 873-884, May 1992.

[14] G. Caire, G. Taricco, and E. Biglieri, "Bit-Interleaved Coded Modulation" IEEE Trans. On Info. Theory, vol. 44, no. 3, May 1998.

[15] D. L. Goeckel, "Adaptive coding for time-varying channels using outdated fading estimates," *IEEE Trans. Commun*., vol. 47, no. 6, pp. 844-855, June 1999.

[16] T. Muller and H. Rohling, "Channel coding for narrow-band Rayleigh fading with robustness against changes in Doppler spread," *IEEE Trans. Commun*., vol. 45, no. 2, pp. 148-151, May 1997.

[17] V. K. N. Lau and M. D. Macleod, "Variable-rate adaptive trellis coded QAM for flat-fading channels," *IEEE Trans. Commun*., vol. 49, no. 9, pp. 1550-1560, May 2001.

[18] A. J. Goldsmith and S. G. Chua, "Adaptive coded modulation for fading channels," *IEEE Trans. Commun*., vol. 46, no. 5, pp. 595-602, May 1998.

[19] P. Ormeci, X. Liu, D. L. Goeckel, and R. D. Wesel, "Adaptive bit-interleaved coded modulation," *IEEE Trans. Commun*., vol. 49, no. 9, pp. 1550-1560, Sep. 2001.

[20] M. S. Alouini and A. Goldsmith, "Capacity of Nakagami Multipath fading channels," in *Proc. IEEE VTC'97*, May 1997, pp. 358-362.

[21] S. T. Chung and A. J. Goldsmith, "Degrees of freedom in adaptive modulation: A unified view," *IEEE Trans. Commun*., vol. 49, no. 9, pp. 1561-1571, Sep. 2001.

[22] X. Qiu and K. Chawla, "On the performance of adaptive modulation in cellular systems," *IEEE Trans. Commun*., vol. 47, no. 6, pp. 884-895, June. 1999.

[23] A. Goldsmith and S. G. Chua, "Variable-rate variable-power MQAM for fading channels," *IEEE Trans. Commun*., vol. 45, no. 10, pp. 1218-1227, Oct. 1997.

[24] V. K. N. Lau and S. V. Maric, "Variable rate adaptive modulation for DS-CDMA," *IEEE Trans. Commun*., vol. 47, no. 4, pp. 577-589, April. 1999.

[25] K. Balachandran, S. R. Kadaba, and S. Nanda, "Channel quality estimation and rate adaptation for cellular mobile radio," *IEEE Jor. Selct. Areas Commun*., vol. 17, no. 7, pp. 1244-1256, July. 1999.

[26] M. Turkboylari and G. L. Stuber, "An efficient algorithm for estimating the signal-to-interference ratio in TDMA cellular systems," *IEEE Trans. Commun*., vol. 46, no. 6, pp. 728-731, July 1998.

[27] D. Falconer, F. Adachi, and B. Gudmundson, "Time division multiple access methods for wireless personal communications," *IEEE Commun. Mag*., vol. 33, no. 1, pp. 50-57, July 1995.

[28] D. A. Gray, "A broadband wireless access system at 28 GHz," in *Proc. Wireless Commun. Conf*., pp. 1-7, Aug. 1997.

[29] B. D. Woerner, J. H. Reed, and T. S. Rappaport, "Simulation issues for future wireless modems," in *IEEE Commun. Mag*., vol. 32, no. 7, pp. 42-53, July. 1994.

[30] A. Kajiwara, "LMDS radio channel obstructed by foliage," in *IEEE Inter. Conf. Coomun*., vol. 3, pp. 1583-1587, June 2000.

[31] K. W. Yip and T. S. Ng, "Discrete-time model for digital communications over a frequency-selective Rician fading WSSUS channel," in *IEE Proc. Commun*., vol. 143, no. 1, Feb. 1996.

[32] F. Hansen and F. I. Meno, "Mobile fading-Rayleigh and Lognormal Superimposed," in *IEEE Trans. Veh. Tech*., vol. 26, no. 4, pp. 332-335, Nov. 1977.

[33] S. Q. Gong and D. Falconer, "Co-channel interference in cellular fixed broadband access systems with directional antennas," in Kluwer Wireless Per. Commun., pp. 103-117, 1998.

[34] T. S. Rappaport and V. Fung, "Simulation of bit error performance of FSK, BPSK, and $\pi/4$ DQPSK in flat fading indoor radio channels using a measurement-based channel model," in *IEEE Trans. Veh. Tech*., vol. 40, no. 4, pp. 731-740, Nov. 1991.

[35] V. Fung, T. S. Rappaport, and B. Thoma, "Bit error simulation for $\pi/4$ DQPSK mobile radio communications using two-ray and measurement-based impulse response models," in *IEEE Jor. Select. Areas Commun*., vol. 11, no. 3, April 1993.

[36] Takashi Kitsuregawa, "Advanced Technology in Satellite Communication Antennas, Electrical and Mechanical Design", *Artech House*; TK7871.6 A39

[37] Salina Q. Gong, "Outage Performance with Directional Antennas in Cellular Fixed Broadband Access Systems", *M.Eng Thesis, Carleton University*, Ottawa, Canada, OCIEE-97-01.

[38] G. Caire, G. Taricco, and E. Biglieri, "Bit-interleaved coded modulation," *IEEE Trans. Info. Theory*, vol. 44, no. 3, pp. 927-946, May 1998.

[39] J. Banks, J. Carson, and B. Nelson, "Discrete-Event System Simulation," *P.T.R. Prentice Hall*, Second Edition, p.536, 1999.

[40] J. Proakis, "Digital Communications," McGraw-Hill Series in Electrical and Computer Engineering, Third Edition, 1995.